

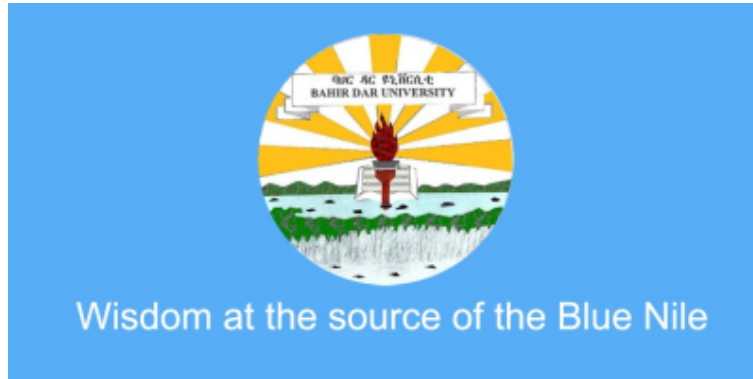
2018-07-18

Temporal and spatial variation of ionospheric total electron content over East Africa GPS receiver network during maximum solar activity period

Tsedal, Mersha

<http://hdl.handle.net/123456789/8898>

Downloaded from DSpace Repository, DSpace Institution's institutional repository



Temporal and spatial variation of ionospheric total
electron content over East Africa GPS receiver network
during maximum solar activity period

Tsedal Mersha

Advisor: Tsegaye Kassa (PhD)

Bahir Dar

Bahir Dar University

June, 2018

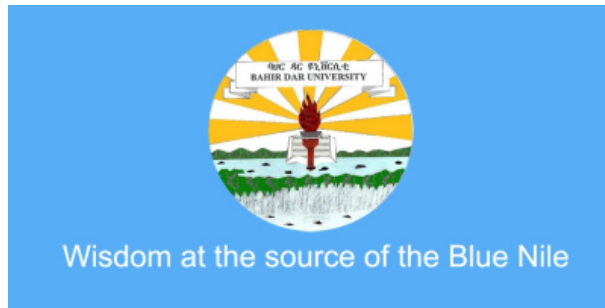
CERTIFICATION

The undersigned hereby certify that they have read and recommend to the school of postgraduate studies for the acceptance of this project work entitled: **”Temporal and spatial variation of ionospheric total electron content Over East Africa GPS receiver network during maximum solar activity period** by **Tsedal Mersha** in Partial Fulfillment of the Requirements for the Degree of **MASTER OF SCIENCE IN PHYSICS** at Bahir Dar University.

APPROVED BY:

Tsegaye Kassa (PhD), Supervisor

Temporal and spatial variation of ionospheric total
electron content over East Africa GPS receiver network
during maximum solar activity period



A Thesis Presented to the School of Postgraduate
Studies Bahir Dar University in Partial Fulfillment of
the Requirements for the Degree of MASTER OF
SCIENCE IN PHYSICS

BY

Tsedal Mersha

Advisor: Tsegaye Kassa (PhD)

June, 2018

AUTHORIZATION TO COPY

Tsedal Mersha hereby authorize the Bahir Dar University to copy and/or release the whole, part of this research work to other researchers and organizations wishing to use the material for reference and/or research purposes.

ACKNOWLEDGEMENTS

First of all I would like to thank GOD for helping me all the way throughout this thesis. Next, I would like to extend my sincere thanks and appreciation to my supervisor Dr. Tsegaye Kassa for his encouragement throughout my thesis work. I am also thanks to Habtamu Wubie for his constant support in programming and computations. My great thanks also goes to Dr. Melessew Nigussie and Fasil Tesema for their encouragement through giving me a feedback of my thesis. I would like to express my sincere gratitude to my lovely brother Aleksander Mersha who supported, encouraged and advised me starting from my undergraduate education life up to now. I am also deeply thanks from my heart Dasash Maregu for her help during data downloading time. My thank is also extend to Habtework Mersha and Bikis Misgan for their treatments throughout this work. Finally, especial thanks goes to my parent who have been offering everything in my whole education life.

TABLE OF CONTENTS

	Page
ACKNOWLEDGMENTS	v
TABLE OF CONTENTS	vi
LIST OF FIGURES	ix
ABSTRACT	xii
Chapter	
1 INTRODUCTION	1
1.1 Background of the Study	1
1.2 Statement of the problem	4
1.3 Objectives	5
1.4 Significance of the study	5
1.5 Thesis overview	6
2 The Sun and Neutral atmosphere	7
2.1 The Sun	7
2.1.1 Sun's interior	7
2.1.2 The Sun atmosphere	9
2.1.2.1 Photosphere	9
2.1.2.2 Chromosphere	11

2.1.2.3	Corona	12
2.2	Earth's Atmosphere	14
2.2.1	Composition of Earth's atmosphere	14
2.2.2	Structure of Earth's atmosphere	15
2.3	Earth's ionosphere	18
2.3.1	Formation of ionosphere	18
2.3.2	Ionospheric Layers	19
2.3.2.1	D layer	19
2.3.2.2	E Layer	20
2.3.2.3	F Layer	21
2.3.3	Ionospheric variability	22
2.3.3.1	Diurnal variation	22
2.3.3.2	Seasonal variation	23
2.3.3.3	Latitudinal variation	24
2.3.3.4	Solar cycle Variation	25
2.4	Geographical region of the ionosphere	25
2.4.1	Equatorial ionosphere	25
2.4.2	Mid latitude	27
2.4.3	High latitude	28
2.5	Ionospheric disturbances	29
2.5.1	Ionospheric storm	29

2.5.2	Geomagnetic storm	29
3	Data and Methodologies	32
3.1	Data source	32
3.2	Method of analysis	33
3.2.1	Estimation of Ionospheric Total Electron Content from dual frequency GPS receiver	34
4	Result and Discussion	37
4.1	Introduction	37
4.2	Diurnal Variation of vTEC	37
4.3	Day to day variability of vTEC	39
4.4	Monthly variation of vTEC	42
4.5	Seasonal variation of vTEC	45
4.6	Latitudinal variation of ionospheric vTEC	48
5	Conclusions and Recommendations	56
5.1	Conclusion	56
5.2	Recommendation	57

List of Figures

2.1	Layer and atmosphere of the sun (adapted from https://www.google.com)	9
2.2	Temperature and density profiles in the solar atmosphere (adapted from Brekke (1997))	13
2.3	Thermal structure of the Earth's atmosphere (Source: https://www. google.com) .	16
2.4	Formation of the Earth's ionosphere (Source: Nigussie, 2013).	19
2.5	Ionospheric ion density profile for the daytime mid-latitude ionosphere showing the layered structure ((Banks et al., 1976)).	20
2.6	Vertical structure of Earth's ionosphere (Source Hargreaves, 1992).	23
2.7	Major geographic regions of the ionosphere (Bishop et al., 1991).	26
2.8	Asymmetry of the Equatorial Ionization Anomaly. E denotes an eastward electric field and B is the northward geomagnetic field (adapted from https://www. google.com).	27
2.9	Vertical plasma drifts due to the meridional neutral wind (WM). W_{\parallel} is the meridional wind along the geomagnetic field line (Source: Ja Soon Shim, 2009).	28
2.10	The interaction between solar wind and magnetosphere (adapted from https://www.google.com/search?q=image+on+interaction+between+solar+wind+and+magnetosphere).	31

2.11	Temporal profile of geomagnetic storm observed in Dst index with different phases during maximum solar activity period (Source: Tsurutani, 2000).	31
3.1	Conversion model from slant TEC to vertical TEC in a thin layer assumption for the ionosphere	36
4.1	A typical quiet ($A_p=1$) diurnal variation of vTEC from five different stations located across East Africa region in the year 2016.	38
4.2	Daily diurnal variation of ionospheric vTEC during November and December months over BDMT and DEBK station	40
4.3	Daily diurnal variation of ionospheric vTEC during November and December months over NEGE and KASM station	40
4.4	Daily diurnal variation of ionospheric vTEC during November and December months over ARSH station	41
4.5	Monthly variation of ionospheric vTEC at BDMT and DEBK stations	43
4.6	Monthly variation of vTEC at NEGE and KASM stations	44
4.7	Monthly variation of vTEC at ARSH station	44
4.8	Seasonal variation of vTEC at BDMT and DEBK stations	46
4.9	Seasonal variation of vTEC at NEGE and KASM stations	47
4.10	The diurnal variation of ionospheric vTEC as a function of latitude during 04 January, 2016	48

4.11 Typical quiet days contour plots of the diurnal variations of TEC, drawn as a function of geographic latitude at five stations (DEBK, BDMT, NEGE, ARSH and KASM) for an equinoxial day, 21 October 2016, a winter day, 2 December 2016 and a summer day, 4 June 2016	50
4.12 Diurnal variation of geomagnetic indices on May 7 - 9, 2016	52
4.13 Typical contour plots of the diurnal variations of TEC, drawn as a function of geographic latitude at five stations (DEBK, BDMT, NEGE, ARSH and KASM) during geomagnetic storm	53

Abstract

Ionospheric Total Electron Content (TEC) is the most important parameter of ionosphere which varies with spatially and temporally such as longitudinal, latitudinal, altitudinal, solar and geomagnetic activities. In this thesis, we have analysed the spatio - temporal variation of ionospheric Total Electron Content (TEC) data obtained from the GPS-TEC over the low latitudinal East Africa regions for the period of 2016. Our result showed that the diurnal variation of vTEC values were maximum during the daytime occurred from 10:00 UT to 15:00 UT while its peak values occurred around 12:00 UT and minimum during pre-dawn and after sunset for all stations. The day to day variation is also significant at all stations, particularly its maximum values of vTEC were occurred during day time and minimum during night time. The seasonal variation of ionospheric vTEC maximum during the Equinox months followed by the winter months (December solstice) and minimum during the summer months (June solstice). The variation of vTEC during geomagnetic storm of the May 2016 has also been investigated. Geomagnetic storm doesn't only affect the magnitude of vTEC but it affect the pattern of vTEC.

CHAPTER 1

INTRODUCTION

1.1 Background of the Study

Earth's upper atmosphere plays an important role in ground-based and satellite radio communication and navigation. Above 80 km altitude the atmosphere contains ionized molecules and free electrons in a region called the thermosphere. Within the thermosphere the amount of ionized gas becomes appreciable and forms a region called the ionosphere (Moldwin, 2008).

The ionosphere is a partially ionized region of the Earth's upper atmosphere. It comprises sufficient number of free electrons and positive ions that is electrically neutral and which extends from 50-1000 kms above the Earth's surface (Hunsucker and Hargreaves , 1995). It has a great influence on the satellite navigation and the radio wave communication systems which causes delay of electromagnetic signals passing through it being a dispersive medium (Davies, 1990; Garner et al., 2008). The main sources of ionization are the solar radiations, such as extreme ultra violet (EUV) and X-ray radiations. Once the plasma is produced by these processes, it undergoes chemical reactions with neutrals, diffuses due to the gravitational force and plasma pressure gradients, and is transported via neutral winds and electric fields under the influence of the Earth's magnetic field (Kelley, 1989). The ionization process is mainly due to solar photons

interacting with the atoms and molecules in the ionosphere, which results in the electron being stripped away from the parent atoms and molecules, and creating a number of free negatively charged electrons and positively charged ions. The ionosphere can be the largest source of error in GPS (Global Positioning System) positioning and navigation. The signal from the GPS satellites travels through the ionosphere region on their way to receivers on the surface of the Earth, the number of negatively free electron on this region of the atmosphere affects the propagation of the signals by changing their velocity and direction of motion. The propagation speed of the GPS electromagnetic signals in the ionosphere depends on its electron density.

The ionospheric TEC is the most important ionospheric parameter. It is the integral of electron number density along the line of sight path from the satellite to the receiver which can be measured by GPS receiver networks. The TEC values at the polar station are very small in comparing with the equatorial station. The solar radiation hits Earth's atmosphere directly over the equatorial station. As the solar radiation hits directly into Earth's atmosphere, more charged particles being emitted that causes stronger ionization processes in ionosphere. Stronger ionization processes leads to higher amount of TEC. The variation of the ionospheric TEC is caused by many factors, such as position, time of day, time of the year, and level of solar activity (Galav et al., 2010; Kumar and Singh , 2009). In particular the ionospheric electron density profiles are strongly affected by solar activity (Klobuchar , 1996; Hamzah and Homam , 2015; Negasa et al., 2015). The solar cycle is the nearly periodic 11-year change in the Sun's activity (including changes in the levels of solar radiation) and appearance (changes in the number and size of sunspots). It is also characterized by an increase in the number of **solar flares, corona holes and coronal mass**

ejection. Huge explosions of magnetic field and plasma from the Sun's corona that is blown away from the sun often during strong, long duration solar flares and filament eruptions, known as coronal mass ejections (CMEs). CMEs are the most dangerous and destructive Space Weather events. When the Sun produces CMEs that travel to the Earth they can carry magnetic field of opposite polarity to that of the Earth. CMEs that enter the Earth's magnetic field may cause geomagnetic storms which usually occur in conjunction with ionospheric storms. CMEs are a result of solar wind comes from active parts of the sun. It is a consequence of the geomagnetic storm. A geomagnetic storm is a temporary disturbance of the Earth's magnetosphere associated with solar coronal mass ejections, coronal holes, or solar flares. The frequency of geomagnetic storms increases and decreases with the sunspot cycle (Moldwin, 2008). During strong geomagnetic activity, a large amount of energy is deposited into the high latitude ionosphere. This implies that an enhancement of electric field and currents together at high latitude (Richa et al. , 2011).

Throughout the 11-year sun cycle, sunspots are highly variable in which generally divided into two, namely, solar minimum and solar maximum. A regular period of greatest Sun activity during the 11-year solar cycle is known as Solar maximum. During maximum solar activity, large numbers of sunspots appear and an enhanced solar activity release high energy (Sun's atmosphere emits large amounts of X-rays) which can greatly affect the Earth's global climate. Solar minimum is the period of least solar activity in the 11 year solar cycle of the sun. During this time, solar flare almost non exist (there is little X-ray emission) and EUV radiation also low and number of sunspot are diminishes, and often does not occur for days at a time.

1.2 Statement of the problem

The electron density of the ionosphere changes with the number and dispersion of free electrons released when gas molecules are ionized by the sun's ultraviolet radiation. Many researchers have been studied the variation of TEC using GPS signals at low and Equatorial latitudes over the Africa sector during both low solar activity and high solar activity. For example the variation of TEC and the performance of IRI - 2012(International Reference Ionosphere) from the African sector at Equatorial latitude during low solar activity studied by [Olawepo et al. \(2017\)](#). Their results revealed that the values of TEC are maximum around 1200 LT (Local Time) - 1500 LT and minimum during the sunrise hour of 0600 LT and the seasonal variability of TEC are observed maximum during the equinoxes than those of the solstices. [Oron et al. \(2013\)](#) studied that the ionospheric variation of TEC data taken from the Uganda Equatorial GPS-SCINDA (GPS-Scintillation Network and Decision Aid) network during the ascending solar phase for the years 2010 and 2011. They also reported the diurnal variability of TEC in the Equatorial region shows its maximum afternoon and minimum during morning and the seasonal variability of TEC have shown maximum during Equinox month and minimum during solstice. The pattern of GPS-TEC variability during both high (2012-2013) and low (2008 - 2009) solar activity phase and the comparison of IRI - 2012 TEC with GPS - TEC during the period of 2012 - 2013 presented by [Yekoye \(2015\)](#). He also presented the diurnal variability of VTEC has showed minimum values at around 0300 UT (Universal Time) (0600 LT) and maximum values nearly between 1000 and 1300 UT (1300 and 1600 LT) during both the low and the high activity while the seasonal variability of VTEC values has observed maxima and minima in March equinox and June solstice,

respectively during both high and low solar activity. Spatio-temporal characteristics of the Equatorial Ionization Anomaly (EIA) in the East African region via ionospheric tomography during the year 2012 investigated by [Kassa et al. \(2015\)](#). They found that the magnitude of the peak and the width/thickness of the EIA pronounced during the equinox and weakened during the solstice seasons at 2100 LT. It is also observed that the EIA persisted for longer time in equinox season than the solstice season. But they have concentrated on the variability of vTEC in terms of daily, hourly and seasonal variation of vTEC and the low latitudinal and equatorial region is very complex and dynamic environment. However, the aim of this study is to analyse the temporal and spatial variability of ionospheric TEC using GPS network during high solar activity over the East Africa sector in the recent year 2016.

1.3 Objectives

- To analyse the temporal and spatial variation of ionospheric TEC data from the East African low latitudinal regions of GPS network of receivers during maximum solar activity

1.4 Significance of the study

The ionosphere plays a great role in broadcasting, ship and air-craft communication and navigation by reflecting the radio signals back to the receivers. TEC is also the most important parameter of the ionosphere. Understanding the variability of TEC is essential for the operation of many applications including satellite navigation and communication system. Therefore, the

main importance of this study is to address the spatial and temporal variability of ionospheric TEC during high solar activity period.

1.5 Thesis overview

The overview of this thesis is structured as follows. Chapter 1 covers introduction on background of the study, statement of the problem, objective and significance of the study. Chapter 2 describes the basic understanding of the sun, lower and upper Earth's atmosphere. Chapter 3 covers data and methodologies of the study. Chapter 4 describes result and discussion and chapter 5 presents conclusion and recommendation of the study.

CHAPTER 2

The Sun and Neutral atmosphere

2.1 The Sun

Sun is the bright ball of a gaseous at the center of the solar atmosphere, like star and with an effective temperature of about 5800 K and it rotates with a period that increases with latitude from 25 days at the equator to 36 days at poles. Its diameter is about 1.39 million kilometers i.e. 109 times that of Earth, and its mass is 1.989×10^{30} kilograms, (about 330,000 times that of Earth), which accounts for about 99.86% of the total mass of the Solar System. Due to its mass sun is composed of approximately 73% H, 25% He and 2% other trace elements. Sun is the most important source of energy that generated in the core due to thermonuclear reaction and transfers outward by radiation. Because of the high densities, the radiation is absorbed and re-emitted many times on its outward journey. The Sun emits radio waves, X-rays, and energetic particles in addition to visible light. The total solar luminosity is 3.83×10^{33} eng/s (Adolph, , 1985).

2.1.1 Sun's interior

Based on the propagation of energy mechanisms, the sun interior is divided into three main regions: the convection zone, the radiation zone, and the core.

Convection zone

At the distance of about 0.72 R the solar gas becomes opaque to the photons and the energy transport toward the surface is called Convection. It is the process that transports heat through bulk fluid motion. Energy from the outer layer of the Sun is transported by convection to the solar surface where it can radiate out into space. In this region, the solar plasma is not dense enough to transfer the heat energy of the interior outward via radiation.

Radiative zone

The energy generated at the core which is mostly in the form of high-frequency X-rays and Gamma rays flows out into the next spherical layer which is called the radiative layer. The radiative zone extends outward from the outer edge of the core to the interface layer at the base of the convection zone (from 25 of the distance to the surface to 70 of that distance). The radiative zone is characterized by the method of energy transport - radiation. The energy generated in the core is carried by light (photons) that bounces from particle to particle through the radiative zone. Although the photons travel at the speed of light, they bounce so many times through this dense material that an individual photon takes about a million years to finally reach the interface layer.

core

The sun's core is the central region of the sun in which thermonuclear reaction occur and it has high temperature and high density. It has one half of solar mass and one fourth of the solar radius. Virtually all of the sun's energy output is generated in the core.

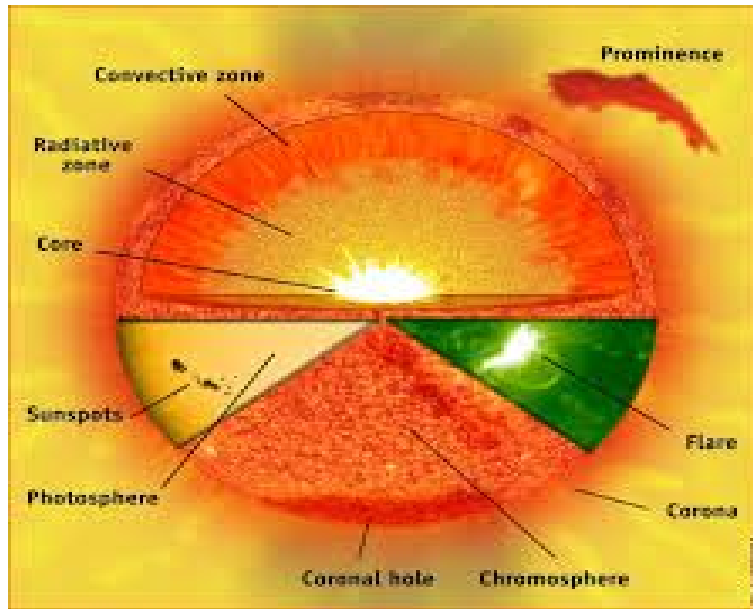


Figure 2.1: Layer and atmosphere of the sun (adapted from <https://www.google.com>)

2.1.2 The Sun atmosphere

The sun's atmosphere is the region of the sun that can be observed from the outside and from which solar energy is radiated into space in the form of kinetic energy of particles, solar wind and solar cosmic rays. It is composed of different layers, namely photosphere, chromosphere, transition zone and corona due to their temperature and densities. Although, there are no boundaries between the layers of the Sun.

2.1.2.1 Photosphere

In the top of the convection zone, in so-called the photosphere which extends to about 500 - 600 km thick. It is the visible surface of the sun. In this region the temperature decreases from 7500

K to 4500 K as well as density also decreases. It is composed of convection cells called granules, and its radiation spectrum is similar to that of a blackbody at 5777 K. Granulation is direct evidence of solar convection. It is the place where sunspot is found. **Sunspots** are temporary phenomena on the photosphere of the Sun that appear as dark spots compared to surrounding regions because they are slightly cooler. They are areas of reduced surface temperature caused by concentrations of magnetic field flux that inhibit convection. It is formed due to the twisted magnetic field lines are hidden below the visible surface. This field lines exerts enormous magnetic pressure on surrounding plasma. As the magnetic pressure being to exceed the plasma pressure, the fields penetrate the surface and appear a bipolar loops. These points of opposite polarity are several thousand degrees cooler than their surroundings and appear as dark spots on the photosphere. Their number varies to approximately 11-year solar cycle. Over the solar cycle, sunspot populations rise quickly and then fall more slowly. The point of highest sunspot activity during a cycle is known as solar maximum, and the point of lowest activity as solar minimum. This period is also observed in most other solar activity and is linked to a variation in the solar magnetic field that changes polarity with this period (Goodman, 2005). Indicating intense magnetic activity, sunspots accompany secondary phenomena such as coronal loops, prominences, and reconnection events. Most solar flares and coronal mass ejections originate in magnetically active regions around visible sunspot groupings. Similar phenomena indirectly observed on stars other than the Sun are commonly called starspots, and both light and dark spots have been measured. Sunspots have two parts: the central umbra, which is the darkest part, where the magnetic field is approximately vertical (normal to the Sun's surface) and the surrounding penumbra, which is

lighter, where the magnetic field is more inclined. The Sun's visible surface is highly mottled, with dark and light regions called granules. Granulation is direct evidence of solar convection. Bright areas show a Doppler blue shift indicating upward motion. Dark areas show a red shift indicating motion down into the solar interior.

2.1.2.2 Chromosphere

The region just above the photosphere is called **the Chromosphere** which is transparent to the visible part of spectrum without strong absorption line and is slightly cooler at its base. It is called chromo because of its color, which can only be seen when the much brighter light from the photosphere is eliminated. When a solar eclipse occurs, the red chromosphere is seen briefly just before and after the period of total eclipse. When viewed in white light, the chromosphere is transparent to the brilliant light emitted underneath it by the photosphere (Brekke, 1997). But when viewed only in the red light produced by hydrogen, the chromosphere is seen to be alive with many distinctive features, including long dark **filaments** and bright areas known as **plage** that surround sunspot regions. The chromosphere is also characterized by cellular convection patterns, but these cells are much larger than the granules of the photosphere. Near the boundaries of these cells are concentrated magnetic fields that produce vertical jets of material called **spicules**. In the chromosphere the temperature is minimum at the top of the photosphere and increases slowly and reaches 9000K at a distance 2000km from the surface of the sun and the density is decrease dramatically. Above the chromosphere is a transition region. In this region

the temperature increases tremendously and reaches a value of 4×10^5 K at 2,500 km above the base of the photosphere.

2.1.2.3 Corona

Outside the transition region the surface of the sun is called corona. It is the hottest part of the solar atmosphere. In this region the temperature is fairly uniform and closed to 10^6 K and the solar atmosphere is fully ionized and it is affected by the solar magnetic field. The coronal's low density accounts for its low luminosity and it is only visible when the bright disk of the sun is occulted during an eclipse by a coronagraph. The solar magnetic field lines extending deep into interplanetary space allow the coronal plasma to escape and these low density coronal area are called coronal holes. It is the main source of high speed solar streams.

Solar flare

Solar flare are strong flashes of x-rays and light energy that shoot off of the sun's surface in to space at the speed of light. The x-rays from flares are stopped by our atmosphere well above the Earth's surface. They do disturb the Earth's ionosphere, however, which in turn disturbs some radio communications.

Coronal Mass Ejections (CMEs)

Coronal mass ejections are the massive clouds of gas and magnetic matter that are eruptions spreading into space. They often follow solar flares and are normally present during a solar prominence eruption. CMEs most often originate from active regions on the Sun's surface, such as groupings of sunspots associated with frequent flares. Near solar maxima, the Sun produces

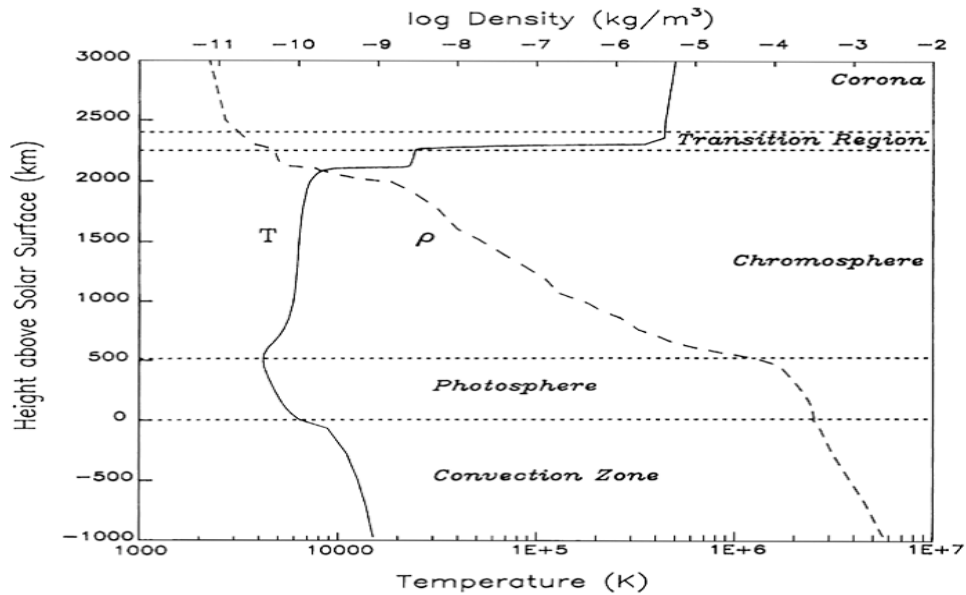


Figure 2.2: Temperature and density profiles in the solar atmosphere (adapted from [Brekke \(1997\)](#))

about three CMEs every day, whereas near solar minima, there is about one CME every five days. Coronal mass ejections are associated with enormous changes and disturbances in the coronal magnetic field. They are usually observed with a white-light coronagraph. When the ejection is directed towards Earth and reaches it as an interplanetary CME (ICME), the shock wave of traveling mass causes a geomagnetic storm that may disrupt Earth’s magnetosphere, compressing it on the day side. When the magnetosphere reconnects on the night side, it releases power on the order of tera watt scale, which is directed back toward Earth’s upper atmosphere. Coronal mass ejections, along with solar flares of other origin, can disrupt radio transmissions and cause damage to satellites and electrical transmission line facilities,

Solar wind

The Sun continuously emits two main types of energy into space electromagnetic (EM) radiation and corpuscular radiation. Visible light, radio waves, microwaves, infrared, ultraviolet, X-rays, and gamma rays are forms of EM radiation. The Sun also continuously emits corpuscular (minute particle) radiation, charged atoms and sub-atomic particles (mostly protons and electrons) in what is called the solar wind. It produces by the temperature difference between the sun's upper atmosphere and the interplanetary space. The solar wind, which expands out into the Solar System carrying with it the Sun's magnetic field, carves out a region of interstellar space called the Interplanetary Magnetic Field (IMF) or heliosphere. The solar wind plasma interacts with the Earth's intrinsic magnetic field and the resulting interaction is important consequence on space systems operating in the near Earth environment. The only visible manifestaion of the interaction is Aurora, which frequently lights up the sky at polar latitudes (both north and south). It varies with the activity of the sun (Moldwin, 2008).

2.2 Earth's Atmosphere

2.2.1 Composition of Earth's atmosphere

The atmosphere of the Earth is the gaseous envelope that covers the earth's surface commonly known as air, which surrounds the planet Earth and is retained by Earth's gravity. It protects life on Earth by creating pressure allowing for liquid water exist on the Earth's surface, absorbing ultraviolet solar radiation, warming the surface through heat retention (greenhouse effect), and reducing temperature extremes between day and night (the diurnal temperature variation). It is

composed of about 78% nitrogen, 21% oxygen and 0.93% argon. The remainder, less than 0.1% contains such trace gases as water vapor, carbon dioxide, and ozone. All these trace gases have important effects on Earth's climate (Kshudiram , 2008).

2.2.2 Structure of Earth's atmosphere

The atmospheric layers of the Earth are characterized by variations in temperature produced by differences in the radiative and chemical composition of the atmosphere at different height. With increasing distance from Earth's surface the chemical composition of air becomes progressively more dependent on altitude and the atmosphere becomes enriched with lighter gases. Based on the temperature change with altitude, the Earth's atmosphere is divided into mainly four concentric spherical strata by narrow transition zones. The four concentric layers of the atmosphere are namely, troposphere, stratosphere, mesosphere and thermosphere. The vertical distribution of temperature in the Earth's atmosphere is as shown in the following.

Troposphere

Troposphere is the lowest layer of the atmosphere and is closest to the Earth's surface, and extends about 8 km above the poles and 18 km over the equator. It contains over 80 of the atmospheric mass and nearly all the water vapor in the atmosphere. The temperature in the troposphere decreases quite monotonically due to the fact that infrared radiation from the ground, which absorbed in the atmosphere and as a result of the decreasing pressure. If a parcel of air moves upwards it expands (because of the lower pressure). When air expands it cools. So air higher up is cooler than air lower down. Water vapor has a major role in regulating air temperature because

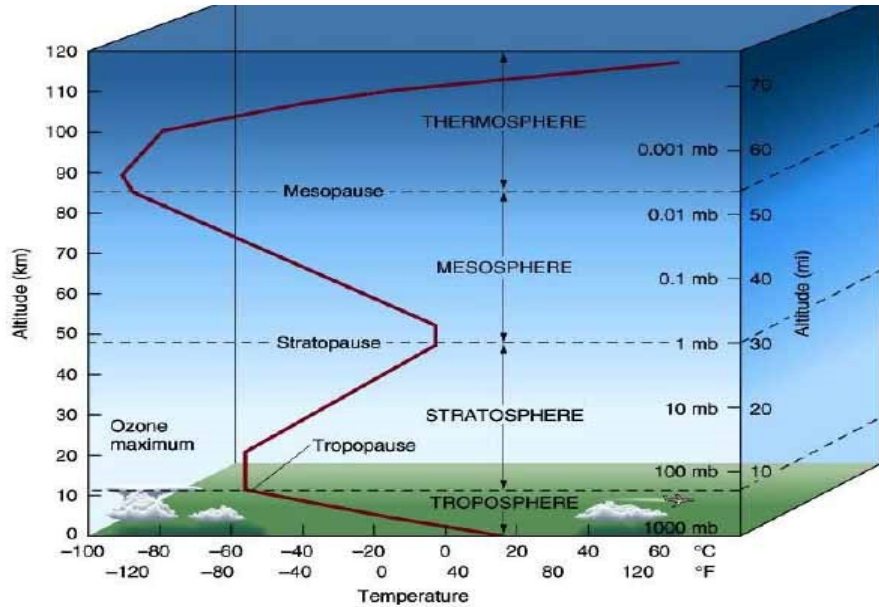


Figure 2.3: Thermal structure of the Earth's atmosphere (Source: <https://www.google.com>)

it absorbs solar energy and thermal radiation from the planet's surface. Troposphere means region of turning or mixing, and is so named because of vigorous convective air currents within the layer. The upper limit of the troposphere is called tropopause. The Tropopause is a thin band located at the top of the troposphere that separates the troposphere from the stratosphere. The temperature remains fairly constant here typically approach $-50^{\circ}C$. This is called also transition zone.

Stratosphere

The stratosphere is the second layer of the atmosphere that extends above tropopause up to 50 km. It contains much of the ozone in the atmosphere. The increase in temperature with height occurs because of absorption of ultraviolet (UV) radiation from the sun by this ozone. As water vapor content within the stratosphere is very low, ozone plays the major role in regulating the

thermal regime of this layer. Based on the ozone layer situated between 5 and 40 km above the ground depending on latitude which absorbs high energy radiation from the sun between 200 and 300 nm, the atmosphere becomes heated in the stratosphere and the temperature increases. The air temperature in the stratosphere increase dramatically to around 273 K at the stratopause. The stratospheric layer is bounded at the top by stratopause.

Mesosphere

It is a layer of the atmosphere that extend from 50 to 80 km and characterized by decrease in temperature with increasing altitude. Because of the concentrations of ozone and water vapor in the mesosphere are negligible as compared with lower regions, hence the lower temperatures. The region is considered to be the coldest of Earth atmosphere reaching a minimum of 180 K at 80 km altitude. The chemical compositions are fairly uniform and pressures are very low. The layer is bounded at the top by the mesopause.

Thermosphere

It is the fourth layer of the atmosphere that extends from the mesopause at an altitude of about 80 km up to the thermopause. The temperature increase is due to the absorption of intense solar radiation by the limited amount of molecular oxygen present. In the thermosphere, the atmosphere is so thin that free electrons can exist for short periods of time before they are captured by a nearby positive ion. The number of these free electrons is sufficient to affect radio propagation. This portion of the atmosphere is partially ionized and contains a plasma which is referred to as the ionosphere (Moldwin, 2008).

2.3 Earth's ionosphere

2.3.1 Formation of ionosphere

Ionosphere is the ionized portion of the upper atmosphere, is an important component of the near-earth space environment. It is a very dynamic environment, and the electron density may significantly vary in time at the given location, which leads to temporal and spatial variations in the Total Electron Content. Because of the solar spectrum deposits its energy at various height depending on the absorption characteristics of the atmosphere, the recombination depending on the atmospheric density (changes with height) and the composition of the atmosphere changes with height (Tascione, 1988). The formation of the ionosphere depends on the activities of the Sun because the main source of ionization and energy for the ionosphere is solar radiation such as extreme ultraviolet (EUV) light and X-ray radiation coming from the Sun. This radiation comes from the sun interacts with neutral atoms giving rise to a number of free negatively charged electrons and positively charged ions is called photoionization process. Because of this process, the ionosphere consists of free electrons and ions. Additionally, the other source of ionization in the ionosphere is impact ionization (energetic particles). In this process the irregularity is formed and have a strong perturbation in radio wave propagation and problems for communications and navigation systems. It formed along the magnetic field lines in the polar region (high latitude). But, in this study we are not concern about the irregularity of ionosphere. Figure 2.5 shows the different ions formed due to ionization of the neutral atoms or molecules at different heights with in the ionosphere.

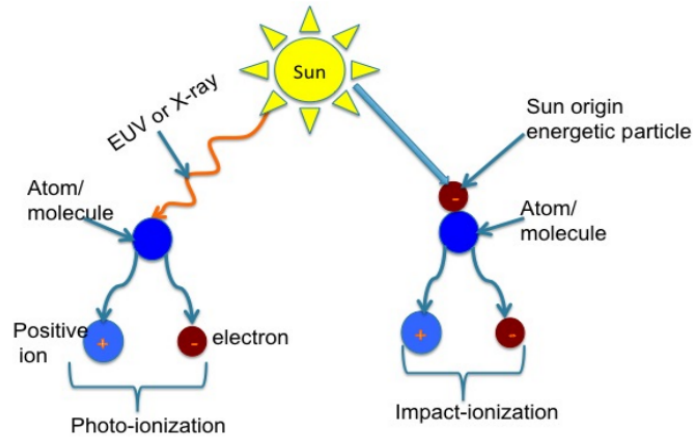


Figure 2.4: Formation of the Earth's ionosphere (Source: Nigussie, 2013).

2.3.2 Ionospheric Layers

Based on the height profile and electron concentration, ionosphere is categorized into four layers, namely, D, E, F1 and F2 layers (Hanslmeier, 2007).

2.3.2.1 D layer

It is the lowest region of the ionosphere, which extends from approximately 60-90 km. The primary source of ionization in this layer is cosmic radiation which is the same by day and by night manifesting itself in a strong solar cycle variation in the D layer electron density. By night, the electrons become attached to atoms and molecules forming negative ions that cause the D layer to diminish in size. The uppermost D layer above 80 km is mainly dominated by NO^+ and O_2^+ ions. The D region electron densities are typically around $10^8 - 10^9 \text{ el}/\text{m}^3$ depending on height. They are subject to typical diurnal, seasonal, and solar-cycle variations. Due to high rate of re-

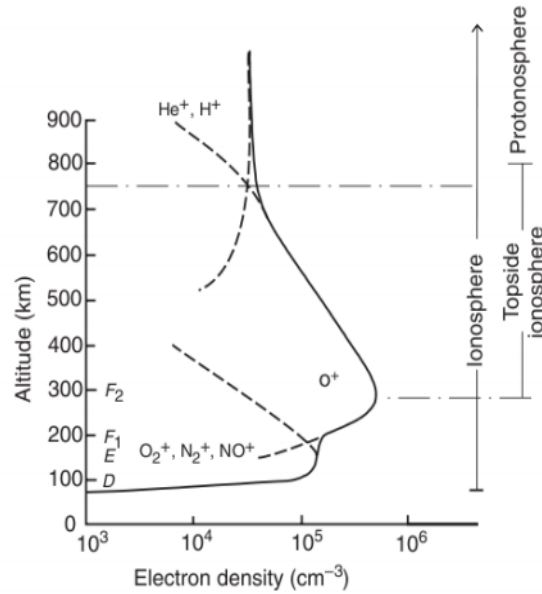


Figure 2.5: Ionospheric ion density profile for the daytime mid-latitude ionosphere showing the layered structure ((Banks et al., 1976)).

combination, in this regions low net ionization occurs. The D region is important with regard to high-frequency (HF) radio communication because it absorbs radio waves, which causes degradation of long-distance HF communication.

2.3.2.2 E Layer

The E layer is the middle layer, which extends about 90 km to 150 km above the surface of the Earth. Ionization is formed by both low energy (or soft) X-rays and UV solar radiation ionization in the range 100 - 150 nm range. The E region is dominated mainly by ionized molecular oxygen (O_2^+) and NO^+ . The vertical structure of the E layer is primarily determined by the

competing effects of ionization and recombination. At night the E layer weakens because the primary source of ionization is no longer present. After sunset an increase in the height of the E layer maximum increases the range to which radio waves can travel by reflection from the layer.

2.3.2.3 F Layer

The F region is a major segment of the terrestrial ionosphere and the most important from the point of view of radio communications and navigation systems. It lies between 150 and 600 km in altitude, occasionally with altitudes extending to the upper limits of the ionosphere. The electron density is highest in the upper, or F region. The F region exists during both daytime and nighttime. During the day it is ionized by solar radiation, during the night by cosmic rays. The F layer divides into two layers during the day because of the enhanced photo-ionization at high altitudes.

F_1 layers

The F_1 layer of the ionosphere lies at an altitude of approximately 150-210 km above the Earth's surface. The ionized component of the F_1 layer consist mostly of NO^+ and O_2^+ and the main source of ionization is extreme ultraviolet (EUV) solar radiation. The height of F_1 varies with solar activity, season, and geomagnetic activity. It exhibits dependence on solar zenith angle χ and sunspot number. The F_1 layer maximum electron density reaching about $2 \times 10^{11} \text{el}/\text{m}^3$

F_2 layer

The F_2 -layer is the most important ionospheric layer from the point of view of HF propagation.

In the F_2 layer the dominant charge carriers are O^+ ions. The main source ionization in the F region is the process of photo-ionization by EUV radiation in the wavelength range from 5 to 102.7 nm. The F_2 layer has a maximum electron density between 10^{10} and $8 \times 10^{12} \text{el}/\text{m}^{-3}$. Because the F_2 layer is a non Chapman layer, there is no solar zenith angle dependence of the diurnal and latitudinal variations in electron density. However, the Sun does affect the electron density of the F_2 layers causing a rapid increase after sunrise, with maximum values occurring at any time during the day. There is also a decrease in the F_2 layer ionization at night, but not as much as the E and D layer ionization. Because, at this higher altitude recombination rates are lower and the layer consists of atomic oxygen rather than the molecular ions that dominate in the D and E regions. This difference in ion behavior is due to the fact that molecular ions have a much higher recombination rate with electrons than do atomic ions (kelley , 2009).

2.3.3 Ionospheric variability

2.3.3.1 Diurnal variation

TEC is highly variable both temporally and spatially. The dominant variability is diurnal following the variation in incident solar radiation because electronic density is related to the solar radiant energy absorbed by the atmosphere and the solar radiant energy is relevant to local time. The absolute value of TEC is maximum during noontime. Higher values of TEC during daytime can be attributed to the increased rate of ionization production due to increased solar radiation intensities coupled with the upward lifting of ionosphere by vertical $E \times B$ drift to higher altitude

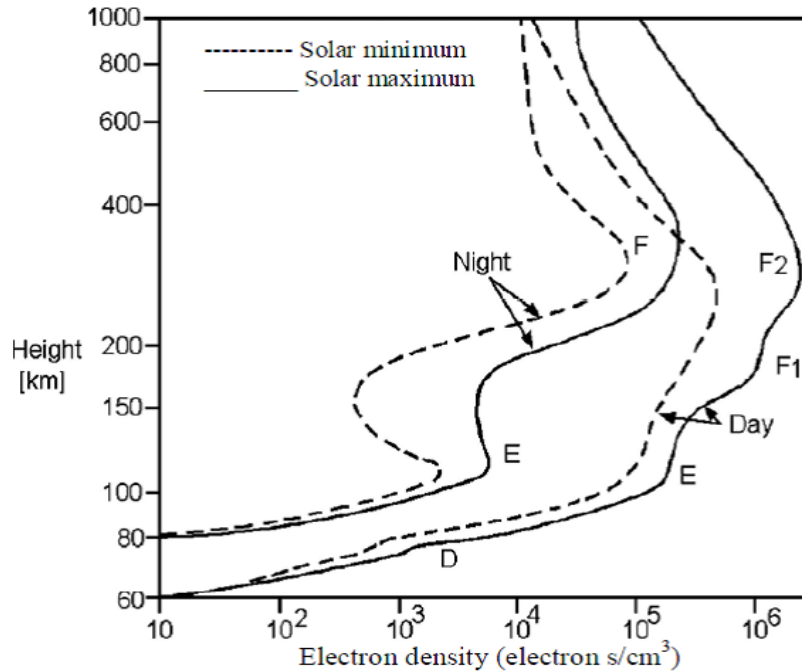


Figure 2.6: Vertical structure of Earth's ionosphere (Source Hargreaves, 1992).

where chemical losses are minimal and also in nighttime the value of TEC is minimum due to the absence of solar radiation, free electron and ions tends to recombine together (Rama Rao et al., 2006; Oron et al., 2013).

2.3.3.2 Seasonal variation

The ionosphere exhibits strong seasonal and solar-cycle variations because the main source of ionization and energy for the ionosphere is photo-ionization. Therefore, whenever either the solar zenith angle or the solar radiations flux change, the ionosphere dynamics may reflect these changes. The ionosphere's seasonal variations is related to solar zenith angle change, while its

solar cycle variation is related to a change in solar EUV and X-ray radiation fluxes. The maximum TEC variability has been found in Equinoxes as compared to the solstices. Because of during equinoxes when the subsolar point is on the equator, meaning that the Sun is exactly overhead at a point on the equator that there is high photo-ionization which produce more electron. Also, during solstices low photo-ionization occur at the equator because the subsolar point moves higher latitudes([Adeniyi , 2008](#); [Adewale et al. , 2011](#))

2.3.3.3 Latitudinal variation

The ionosphere is a function of latitude and the latitudinal response to the variations also depends on the time of the day. At latitude about 20 degrees either side of the geomagnetic equator, high TEC values are produced by a so called fountain effect. The effect is caused by $E \times B$ drifting electrons interacting with the Earth's magnetic field to produce large scale movement of ionization. The equatorial anomaly is formed as a consequence of $E \times B$ upward plasma drifts associated with an eastward E-field and a northward horizontal B-field. The lifted plasma then diffuses downward along the geomagnetic field lines due to the gravitational force and the plasma pressure gradient, and this results in ionization enhancements on both sides of the magnetic equator ($\pm 15^\circ$ in the latitude) ([Opio et al. , 2015](#); [Olwendo et al. , 2012](#)).

2.3.3.4 Solar cycle Variation

The solar cycle is the rise and fall of the number of sunspots on the Sun. Solar activity is correlated to the number of sunspots on the Sun. As the number of sunspots goes up, solar activity occurrences go up. Energy output from the Sun also changes as the sunspot count on the Sun changes. It is greatest when there are the most sunspots and lowest when there are the least sunspots. During solar minimum there is little X-ray emission, while at solar maximum the Sun's atmosphere emits large amounts of X-rays.

2.4 Geographical region of the ionosphere

There are three main region of global ionospheres, namely, low or equatorial latitude, mid latitude and high latitude regions.

2.4.1 Equatorial ionosphere

The equatorial region of the ionosphere, occasionally referred to as the low latitude zone. It is strongly affected by electromagnetic (EM) forces that arise due to the geomagnetic field which runs horizontally over the magnetic equator. The equatorial ionosphere is highly dynamic and consequently poses serious threats to communication and navigation systems. Due to the unique geometry of the magnetic fields at the equatorial and low latitudes, the ionospheric effects on GPS signals are more pronounced in the low latitudes than in the other latitudes. The equatorial and low latitude ionosphere is characterized in terms of latitudinal of ionization by a trough

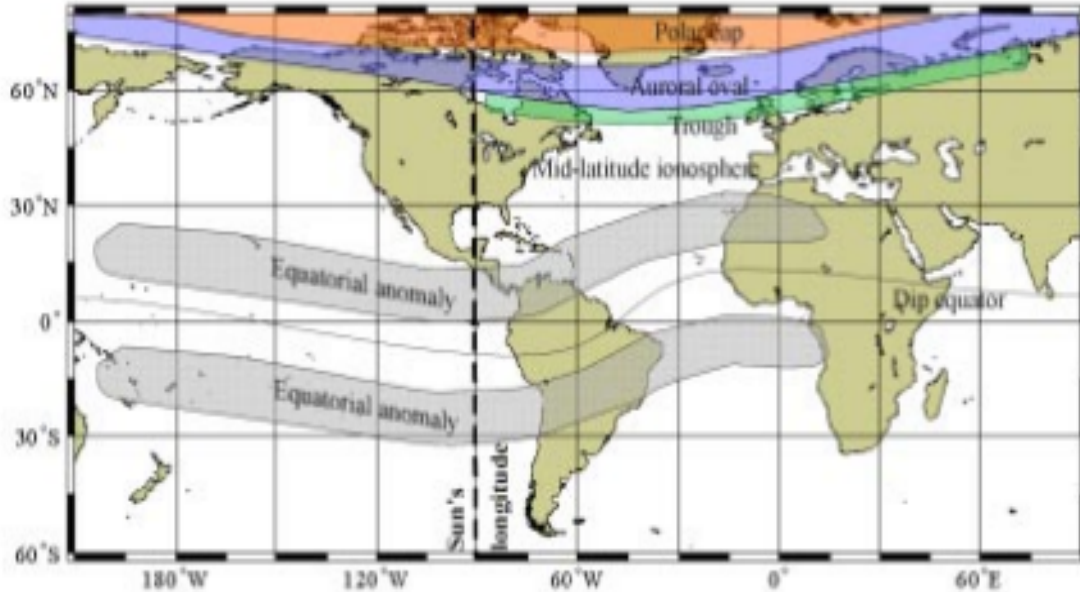


Figure 2.7: Major geographic regions of the ionosphere (Bishop et al., 1991).

at the magnetic equator and crests at about ± 17 magnetic latitude, a feature referred to as the equatorial ionization anomaly (EIA). The cause of the anomaly is often attributed to the so-called fountain effect, whereby an eastward electric field at the equator gives rise to an upward $E \times B$ drift during the daytime. After the plasma is lifted to greater heights it is able to diffuse downward along magnetic field lines under the influence of gravity and pressure gradient forces. In the summer hemisphere, plasma moves upward along the geomagnetic field lines, while plasma moves downward in the winter hemisphere. Therefore the plasma is transported from the summer hemisphere to the winter hemisphere. As result, the equatorial anomaly crests in the winter hemisphere are generally larger than in the summer hemisphere as shown Figure 2.8. Therefore, over the low-latitude zones, the signal degradation may be more likely because of large variations

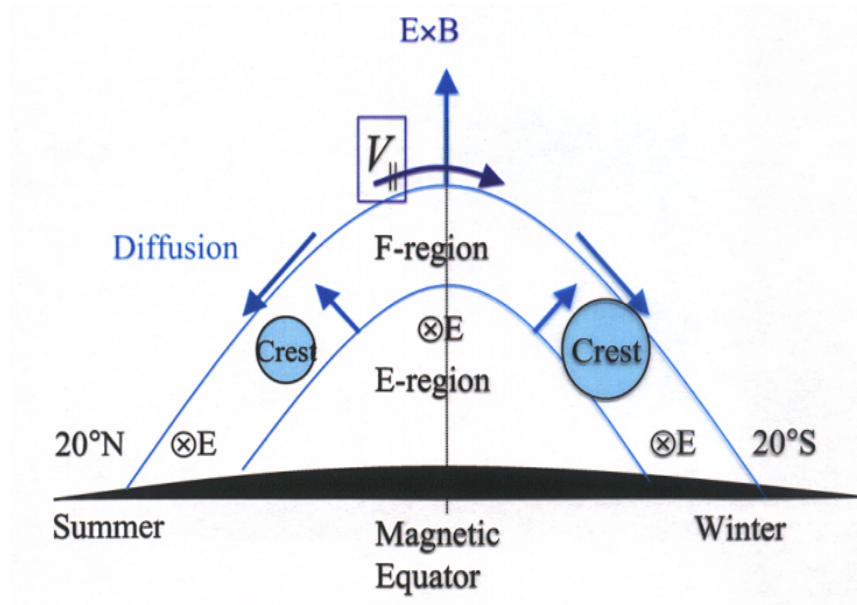


Figure 2.8: Asymmetry of the Equatorial Ionization Anomaly. E denotes an eastward electric field and B is the northward geomagnetic field (adapted from <https://www.google.com>).

of TEC near the crest of EIA owing to very large background TEC values.

2.4.2 Mid latitude

The middle latitude ionosphere is a relatively less variable and disturbed region because of the ionosphere sensing instruments, observations and measurements are best obtained at this region. In this region the transport of plasma are depend on the geomagnetic field line is inclined to the horizontal and the ionospheric plasma is constrained to move along the geomagnetic field lines. Because of the thermospheric neutral wind, the transport of the plasma along the field lines is into the higher or the lower regions in which the recombination rate are different due to change the plasma density.

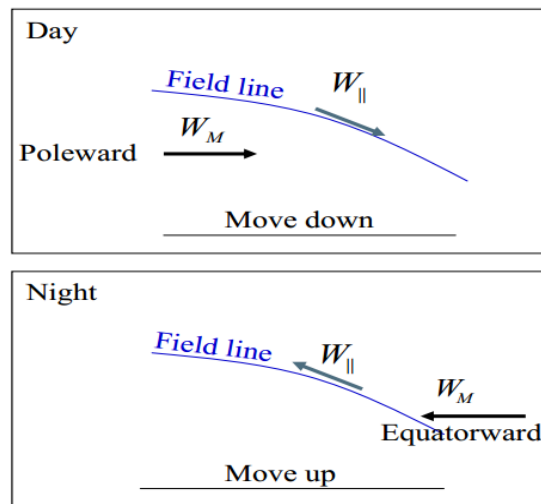


Figure 2.9: Vertical plasma drifts due to the meridional neutral wind (W_M). W_{\parallel} is the meridional wind along the geomagnetic field line (Source: Ja Soon Shim, 2009).

2.4.3 High latitude

In addition to photonization, collisional ionization is another source of ionization in the high-latitude region and at these altitudes the solar radiation is stronger but there are fewer gaseous atoms to interact with, hence ionization is less. The main reason for this is the fact that the geomagnetic field lines are nearly vertical in this region leading to the charged particles descending to E layer altitudes (about 100 km). At high latitudes there is another source of ionization of the ionosphere the aurora. The light of the aurora is caused by high speed electrons and protons, coming from the magnetosphere spiralling down the Earth's magnetic field lines. The aurora form when charged particles emitted from the sun during a solar flare penetrate the earth's magnetic shield and collide with atoms and molecules in our atmosphere. These collisions result in countless little bursts of light, called photons, which make up the aurora. Collisions with oxy-

gen produce red and green auroras, while nitrogen produces the pink and purple colors. It also most commonly occur between 60° - 75° latitude, but during great geomagnetic storms the auroral oval expands equatorially and can reach 30° latitude or further. In the northern hemisphere they are called the aurora borealis (northern lights) and in the southern hemisphere aurora australis (southern lights).

2.5 Ionospheric disturbances

2.5.1 Ionospheric storm

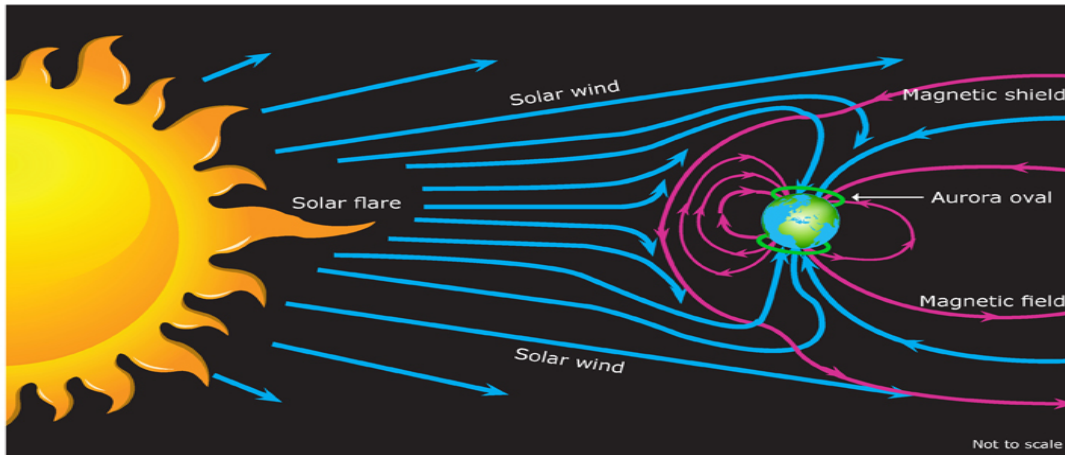
The disturbed ionosphere is also one of the main characteristics responded to the geomagnetic storm. Due to many interacting factors, each storm could show a different course. During geomagnetic storms the electron density can either increase (positive ionospheric storm) or decrease (negative ionospheric storm), and this considerably disturbed behavior is commonly called as the ionospheric storm.

2.5.2 Geomagnetic storm

Geomagnetic storm is the temporal disturbance of the Earth's magnetosphere caused by the sun emits an energetic charged particle like solar flare, coronal mass ejection (CMEs) or solar wind which interacts the Earth's magnetic field and transfers high amount of energy into the Earth's magnetosphere. These reconnection creates an increase electric current inside the magnetosphere (free movement of ions and electrons). As the solar wind collides (interfere) with the magneto-

sphere, its velocity and pressure and its embedded interplanetary magnetic field (IMF) are highly variable due to its origin in different solar active regions. Sudden changes of its parameters, manifested as the occurrence of shock waves and most significantly the southward turning of the IMF Bz component, lead to a rapid increase of magnetic reconnection processes at the magnetopause. When Bz is strongly negative, magnetic reconnection between the IMF and the geomagnetic field produces open field lines which allow mass, energy and momentum to be transferred from the solar wind to the Earth's magnetosphere. This results in dramatic increase of solar wind energy input into all regions of the geosphere system, hence generating geomagnetic storms. Significant geomagnetic disturbances produce awe-inspiring auroral displays in the northern hemisphere (aurora borealis) and in the southern hemisphere (aurora austral), but they can also cause disruptive effects, such as loss of satellites signals and failure of communication network and electric power grids.

Geomagnetic storm has three phases. First, initial phase is characterized by Dst increasing approximately by 20 nT to 50 nT in ten minutes. It is also known as a storm sudden commencement (SSC). Second, main phase is defined by Dst decreasing to less than -50 nT means a storm is somewhat arbitrary. During these time an electric current in the magnetosphere creates a magnetic force that pushes out the boundary between the magnetosphere and the solar wind. The duration of these phase is 2 - 8 hours. Third, recovery phase is when Dst changes from its minimum value to its quiet value. The duration of recovery phase may last as short as 8 hours or as long as 7 days.



© Copyright. 2014. University of Waikato. All rights reserved.
www.sciencelearn.org.nz

Figure 2.10: The interaction between solar wind and magnetosphere (adapted from <https://www.google.com/search?q=image+on+interaction+between+solar+wind+and+magnetosphere>).

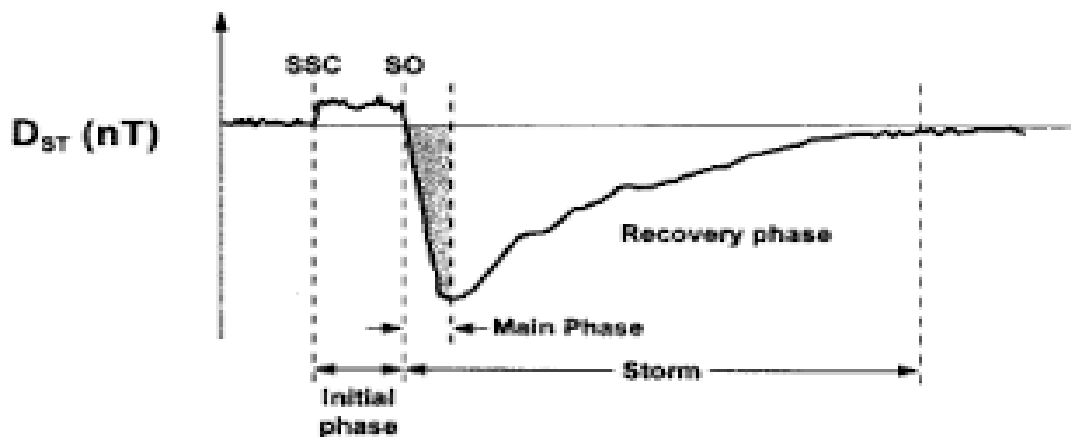


Figure 2.11: Temporal profile of geomagnetic storm observed in Dst index with different phases during maximum solar activity period (Source: Tsurutani, 2000).

CHAPTER 3

Data and Methodologies

3.1 Data source

For this study, we obtained GPS-TEC data from the GPS receiver network at 5 stations over the East African region during maximum solar activity period in the year 2016 using identical dual-frequency GPS receivers . The TEC data are available at UNAVCO (University Navstar Consortium) website (<http://www.unavco.org/>) and the solar wind parameters used for the analysis of this geomagnetic storm were obtained from in the website <http://www.omniweb.gsfc.nasa.gov/>. The Receiver-independent exchange (RINEX) observation obtained from the IGS websit were processed by the GPS-TEC analysis application software. The data from satellites of elevation angle greater than 30° , to eliminate the low elevation angle effects, due to multipath and tropo-scatter, due to water vapor on the measured TEC values (Olowendo et al., 2016; Opio et al. , 2015).

Table 3.1: Geographical Latitudes and Geomagnetic Longitude for Receivers over the East Africa

Region Used in This Study

No	Station Code	Geographical Latitude (deg)	Geographical Longitude (°E)
1	Negele (NEGE)	5.33	39.58
2	Bahir Dar (BDMT)	11.59	37.35
3	Debark (DEBK)	13.15	37.89
4	Arusha (ARSH)	-3.38	36.69
5	Misamfu (KASM)	-10.17	31.22

3.2 Method of analysis

GPS signals that propagate through the ionosphere at two L-band GPS frequencies L1 (1575.42 MHz) and L2 (1227.36 MHz) provides an important ionospheric parameter which is TEC. The TEC is defined as the total number of electrons integrated along the path from the receiver to the GPS satellite in a column with a cross-sectional area of one square meter which is logically evaluated first in terms of its height profile, followed by its spatial and temporal variabilities (Goodman, 2005). GPS receiver measurement is used to calculate the electron density along a ray path between the satellites to the receiver on the ground by utilizing dual frequency and usually expressed in total electron content units (TECU) as:

$$TEC = \int_R^S N_e ds$$

Where $1TECU = 10^{16}e/m^2$ and N_e is the total number of the accumulated electrons in each square meter area through the differential distance (ds) along the path from the satellite to the

receiver on the ground.

The ionospheric time delays (t_1 and t_2) at the L1 (of f_1) and L2 (of f_2) carrier frequencies are given by

$$t_1 = 40.3\left(\frac{TEC}{cf_1^2}\right); t_2 = 40.3\left(\frac{TEC}{cf_2^2}\right) \quad (3.1)$$

where 'c' is the speed of light in free space. The difference in delay time between the two frequencies, $\Delta t = t_2 - t_1$ is given by

$$\Delta t = \left(\frac{40.3}{c}\right) \times TEC \times \left(\frac{1}{f_2^2} - \frac{1}{f_1^2}\right) \quad (3.2)$$

3.2.1 Estimation of Ionospheric Total Electron Content from dual frequency GPS receiver

The ionosphere is a dispersive medium, which means that the apparent time delay contributed by the ionosphere depends on the frequency of the signal. One of the most fundamental GPS observables is C/A (Coarse Acquisition) code pseudorange which is generally used for standard positioning. The code pseudorange is measured from propagation time of the signal from i^{th} satellite to the receiver and is represented by

$$R^i = \rho^i + c(\delta t_r - \delta t_s^i) + \delta_{ion}^i + \delta_{tro}^i + \varepsilon \quad (3.3)$$

Where ρ^i is the geometric distance between satellite and receiver, c is the speed of light, δt_r and δt_s^i are the transmitting and the receiving time error, respectively, δ_{ion}^i and δ_{tro}^i are the ionosphere and tropospheric effects along the propagation path of the signal, respectively, and ε denotes other effect, like, multipath effect and receiver noise.

The ionospheric delay δ_{ion}^i is directly proportional to the total electron content (TEC) from the i^{th} satellite to the receiver. This is called slant TEC and denoted by I_{slant}^i .

$$\delta_{ion}^i = \frac{e^2}{8\pi^2 m \varepsilon_o c f^2} I_{slant}^i = \frac{I_{slant}^i}{\Lambda} \quad (3.4)$$

Where e, m, ε_o and f are charge of the electron, mass of the electron, permittivity of free space and the signal frequency, respectively and $\Lambda = \frac{8\pi^2 m \varepsilon_o c f^2}{e^2}$.

From Equ. (3.3) and (3.4), the slant TEC is calculated as

$$I_{slant}^i = \Lambda(R^i - \rho^i + c\delta t_s^i - \delta_{tro}^i) - \Lambda c\delta t_r + \varepsilon \quad (3.5)$$

Since the ionospheric TEC distribution is usually shown by vertical TEC map, the slant TEC is converted to vertical TEC (vTEC) by a slant factor. The ionosphere can be assumed to be a thin layer and the ray path crosses the ionosphere at one point called the ionospheric pierce point (IPP) as shown in the figure below.

From Figure 3.1 the conversion method from slant TEC I_{slant}^i to vertical TEC $I_{vertical}^i$ can be used as follows;

$$\begin{aligned} \cos(\chi) &= \frac{I_{vertical}^i}{I_{slant}^i} \\ I_{slant}^i &= I_{vertical}^i \cdot \frac{1}{\cos(\chi)} \end{aligned} \quad (3.6)$$

where the angle χ between zenith direction and satellite direction from the IPP and by using sine triangle law can be calculated as follows;

$$\chi^i = \sin^{-1}\left(\frac{R_E}{R_E + h} \cos \theta_{el}^i\right) \quad (3.7)$$

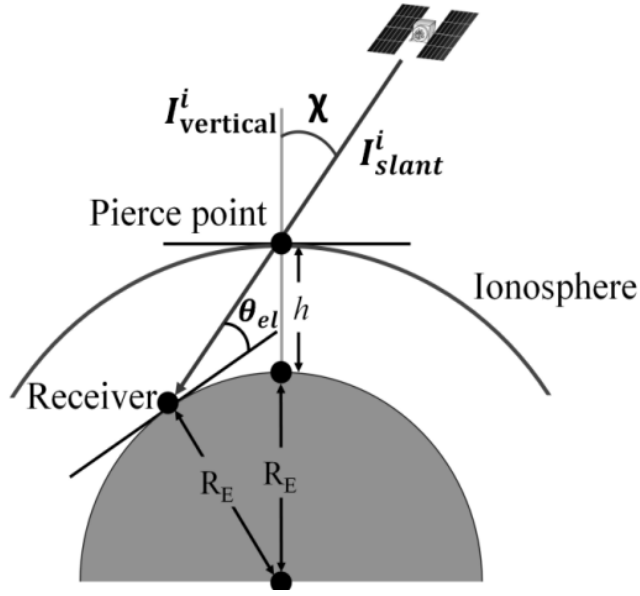


Figure 3.1: Conversion model from slant TEC to vertical TEC in a thin layer assumption for the ionosphere

Where R_E is Earth radius, h is the height of IPP and $\cos \theta_{el}^i$ is elevation angle of the satellite at the receiver location.

Therefore, from Eq. (3.5), (3.6) and (3.7), vertical TEC can be calculated by

$$vTEC = (k - a) \cos \chi \quad (3.8)$$

Where $k = \Lambda(R^i - \rho^i + c\delta t_s^i - \delta t_{tro}^i)$ and $a = \Lambda c\delta t_r$ (Win et al., 2016).

After that we use MATLAB software and we plot our data.

CHAPTER 4

Result and Discussion

4.1 Introduction

In this chapter we are going to analyse the spatio temporal variation of ionospheric $vTEC$ over the East African regions in the year 2016. The temporal variation was investigated in terms of diurnal, daily, monthly and seasonal variation of $vTEC$. Also, the spatial variation were analysed in terms of latitudinal variation of $vTEC$. In the following section we present the main findings of our result.

4.2 Diurnal Variation of $vTEC$

Figure 4.1 illustrates a typical quiet ($A_p=1$) diurnal variation of $vTEC$ from five different East African regions in the year 2016. The left panel of these Fig. depicts a typical diurnal variation of $vTEC$ during October 20 (top) and November 19 (bottom). It is clearly shows that the maximum $vTEC$ values were observed near the magnetic equator (ARSH, NEGE, DEBK and BDMT), respectively while least values of $vTEC$ were registered at KASM station. The right panel of these Fig. demonstrates the typical diurnal variation of $vTEC$ in December 16 and 19 at the

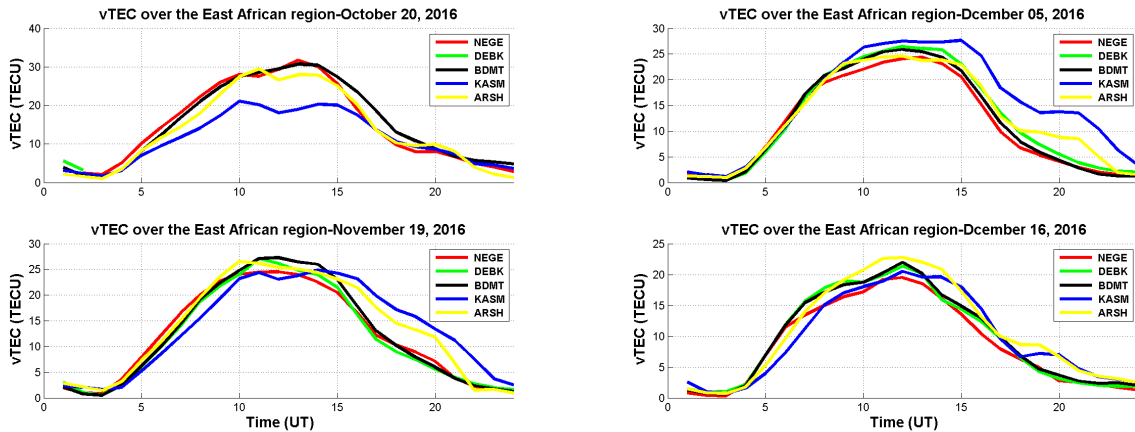


Figure 4.1: A typical quiet ($A_p=1$) diurnal variation of $vTEC$ from five different stations located across East Africa region in the year 2016.

top and the bottom, respectively. As we can see this, its peak $vTEC$ values were recorded at KASM (top) and ARSH (bottom) while the minimum values of $vTEC$ observed at NEGE station. In addition, from these it can conclude that the maximum values of $vTEC$ were mostly occurred around from 10:00 UT to 15:00 UT at daytime, while their values were decreases in the nighttime hours and becomes minimum after midnight hours mostly around from 00:00 - 03:00 UT. This indicates that the day time values of $vTEC$ are greater than the nighttime values of $vTEC$. This observations can be attributed to the fact that the main source of ionization in the ionosphere can depends primarily on the activity of the Sun. The amount of ionization in the ionosphere varies greatly with the amount of solar radiation coming from the Sun. As the sun rises, the ionization also increases which causes more concentration of electron near the F_2 peak at the ionosphere. According to [Kassa et al. \(2017\)](#), the daytime maximum value of $vTEC$ is an indication of the dominant role played by the production component due to increase in solar EUV radiation during

the daytime in all days while the minimum values of vTEC observed during the nighttime in all days can be attribute to the leading role of the recombination process. The plasma distribution in the low and equatorial latitude is depends on the thermospheric neutral wind, vertical $E \times B$ drift and the field aligned diffusion ([Opio et al. , 2015](#)). In general, the diurnal variation of vTEC show a pre-dawn minimum, a steady early morning increase, followed by afternoon maximum and gradual fall after sunset. This observations are in agreement with previous studies ([Olawepo et al., 2017](#); [Ratnam et al. , 2017](#)). The observation of diurnal variation of vTEC shows that the time at which vTEC reaches the diurnal peak vary from day to day and month to month.

4.3 Day to day variability of vTEC

In order to analyse the daily variation of vTEC over five stations in East Africa in the year 2016 during November and December months, the daily averaged value of vTEC has been calculated. However, in this study the month of January to October are not presented for all stations due to incompleteness of 24h GPS data. The contour plot of the daily diurnal variability of vTEC over five East Africa regions during November and December are illustrated in [Fig. 4.2 - 4.4](#).

Figure [4.2](#) shows the daily diurnal variation of ionospheric vTEC over BDMT and DEBK stations during November and December months. As it can be seen from the figure, the left panel indicates the daily variation of vTEC on BDMT station and its maximum vTEC values obtained approximately around 35 (TECU) from 11:00 UT to 14:00 UT on November 4 - 6 while its maximum vTEC values reached approximately around 30 (TECU) during at the beginning

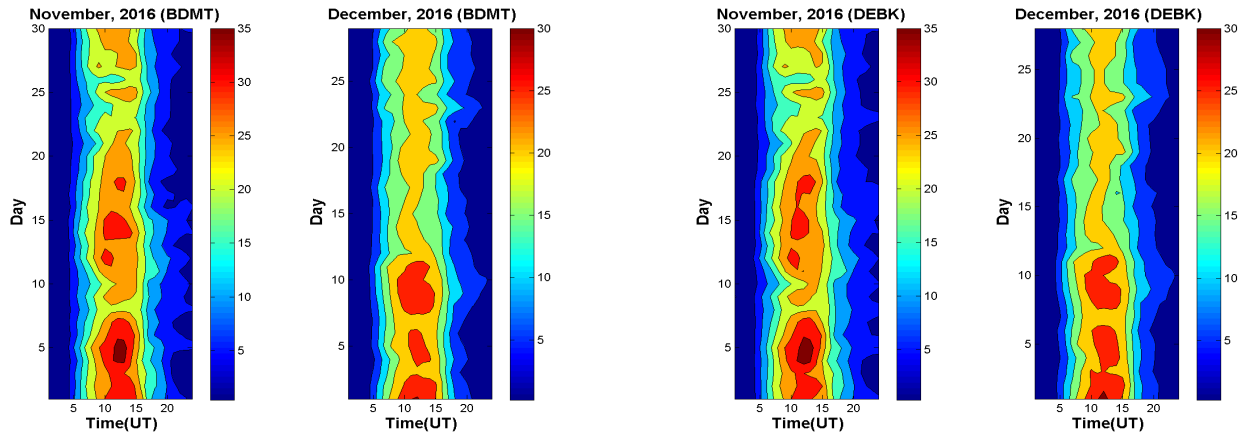


Figure 4.2: Daily diurnal variation of ionospheric vTEC during November and December months over BDMT and DEBK station

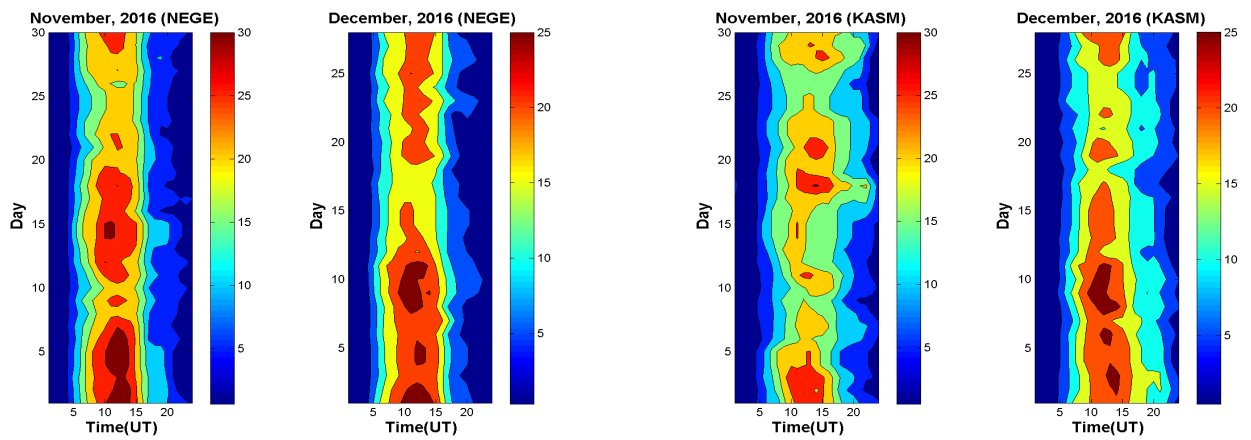


Figure 4.3: Daily diurnal variation of ionospheric vTEC during November and December months over NEGE and KASM station

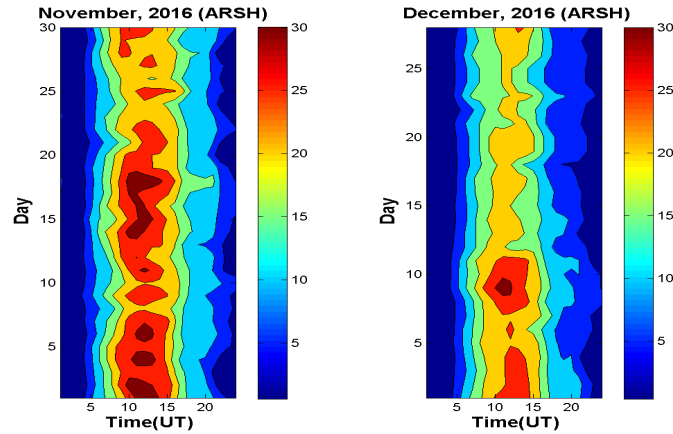


Figure 4.4: Daily diurnal variation of ionospheric vTEC during November and December months over ARSH station

of the December month at around 12:00 UT. Also, the right panel represents the daily variation of vTEC at DEBK station, the maximum value of vTEC attained around 11:00 - 14:00 UT at about 35 (TECU) during December 4- 6 while during November month the maximum vTEC occurs from 11:00 - 13:00 UT approximately around 30 (TECU) at the beginning of these month. From Fig 4.3 we can see that the daily diurnal variation of vTEC over NEGE and KASM stations during November and December months. As it is clearly see in the figure, the left panel represents the daily variation of vTEC at NEGE station. Its peak vTEC values occurs around from 10:00 - 14:00 UT and its maximum value reached approximately 30 TECU on November 1-7 and 14 while during December the maximum vTEC observed from 10:00 - 15:00 UT approximately 25 (TECU) at the beginning of this month. The right panel shows the daily variation of vTEC at KASM station, the maximum vTEC occurs around at 14:00 UT and its maximum values reached at about 30 (TECU) on November 17 while the maximum vTEC occurs nearly between 10:00

- 14:00 UT and its peak values observed approximately around 20 (TECU) on December 2, 3, 6 and 8-12. The daily diurnal variation of vTEC during November and December at ARSH station shown in Figure 4.4. As observed from these Fig. the maximum variation of vTEC occurs nearly between 9:00 - 14:00 UT and its maximum values reached approximately 30 (TECU) on November 1, 2, 4, 6,11, and 14 - 18 while the maximum variation of vTEC occurs around 11:00 - 12:00 UT and its maximum values recorded at about 30 (TECU) on December 9. In all these plots the diurnal daily variations show a maximum occurring around 09:00 - 15:00 UT and short-lived minimum in vTEC occurs nearly between 00:00 to 8:00 UT and 16:00 - 23:00 UT and . According to Yinn et al. (1989),Malini et al. (2012) and Richa et al. (2011), the day to day variability of TEC is contributed by the various parameters like solar EUV radiation and geomagnetic activity which is associated with the changes in the intensity of the incoming radiation at which the radiation is incident at the Earth's atmosphere, since the intensity increases starting from sunrise and becoming maximum when Sun is overhead and comes to zero when sunset. In low latitude regions, the highest daytime peak vTEC values depend greatly on the strength of the equatorial ionization anomaly (EIA). During the daytime, the tide wind and zonal neutral wind generates an eastward electric field that is responsible for the formation of the EIA.

4.4 Monthly variation of vTEC

In order to estimate the monthly variation of vTEC from January to December 2016 over East Africa sector, the monthly mean variation of vTEC has been calculated and it is portrayed by

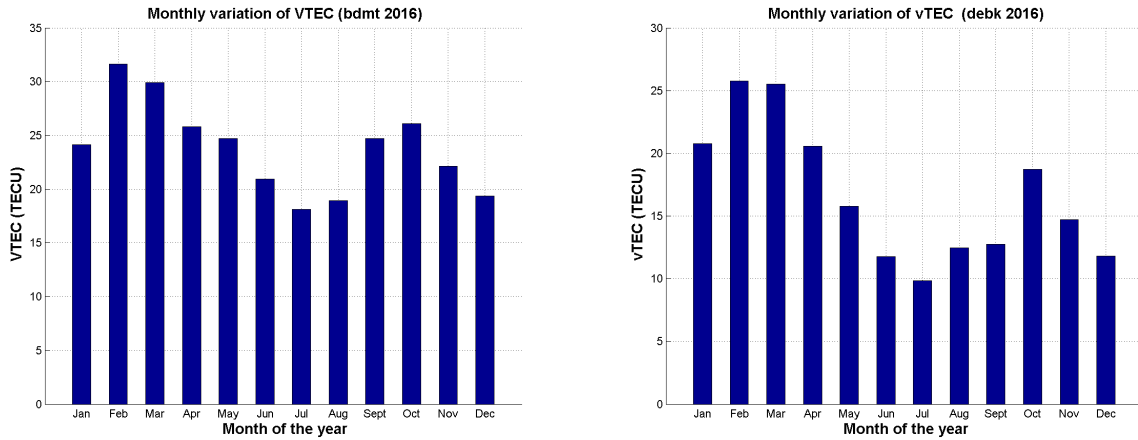


Figure 4.5: Monthly variation of ionospheric vTEC at BDMT and DEBK stations

Figures 4.5 - 4.7 . However, for KASM station, the data of January to April 20 and for ARSH station April 5 to June 20 were missed. The left and right panels of Figure 4.5 shows the monthly variation of ionospheric vTEC over BDMT and DEBK stations, respectively. The left panel of these Fig. represents the monthly variation of vTEC over BDMT station, its peak vTEC values were recorded in February month approximately at about 32 (TECU) while the last minimum values of vTEC observed during July approximately around 19(TECU). The right panel of Fig.4.5 depicts the monthly variation of vTEC over DEBK station. As it is clearly see in the figure the maximum vTEC values observed in February approximately 26 (TECU) and the minimum vTEC values were recorded in July around 10 (TECU). Figure 4.6 represents the monthly variation of vTEC at NEGE and KASM stations. As we can see from the left panel of these Fig. the maximum vTEC values was observed during March approximately 24 (TECU) and the minimum values of vTEC observed in July at NEGE and it is at about 11 (TECU). From the right panel of Fig. 4.6, the peak values of vTEC was observed in October approximately 17 (TECU) and the last

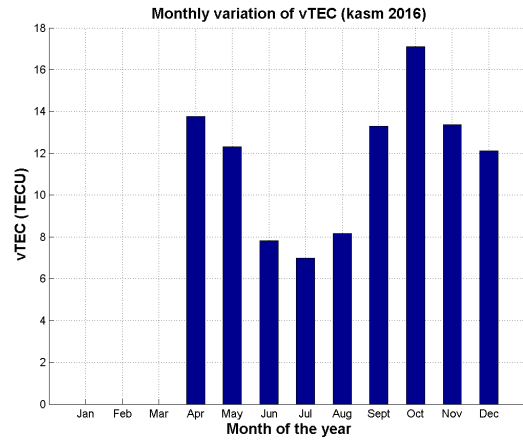
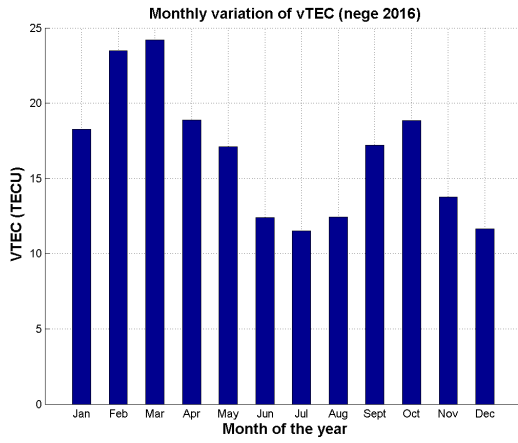


Figure 4.6: Monthly variation of vTEC at NEGE and KASM stations

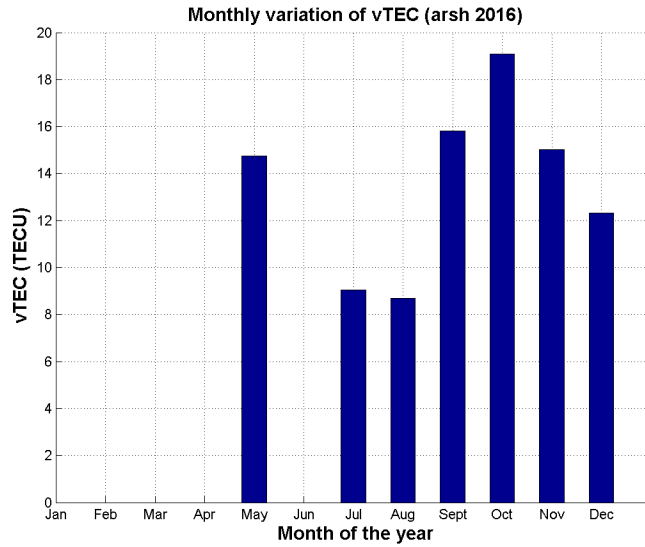


Figure 4.7: Monthly variation of vTEC at ARSH station

minimum vTEC values observed in July at about 11 (TECU) over Kasm station. As shown Fig 4.7, the peak vTEC values were observed in October approximately 19 (TECU) while the last vTEC values observed in August approximately 9 (TECU) at ARSH station. The result shows that the maximum value of vTEC were observed in February month ≈ 32 TECU and ≈ 26 TECU over BDMT and DEBK stations respectively , the two stations in the northern hemisphere than the other remaining stations. It has also been shown that the maximum monthly vTEC values were observed in the march equinox while the last monthly vTEC values observed in the June solstices. Hence from these it can be conclude that the variability of vTEC mainly depends on the intensity of radiations coming from the sun, since in equinox month the sun becomes over head and it has maximum photo-ionization and maximum value of vTEC. During solstices months, the earth is far away from the point of the sun, the value of vTEC is then not significant.

4.5 Seasonal variation of vTEC

The seasonal variation of vTEC are illustrated in Figure 4.8 and 4.9. However, for ARSH station, the seasonal variation of vTEC is not presented due to lack of full GPS-TEC data. As shown in these figure, the whole years are categorized into four seasons such as, March Equinox (February, March, April), September Equinox(August, September and October), December solstices (November, December and January) and June solstices(May, June and July). To investigate the seasonal variation of vTEC, to calculate for all day of seasons mean values of vTEC and we used an elevation angle of 30° for all GPS data to eliminate the effect of clock errors, tropospheric

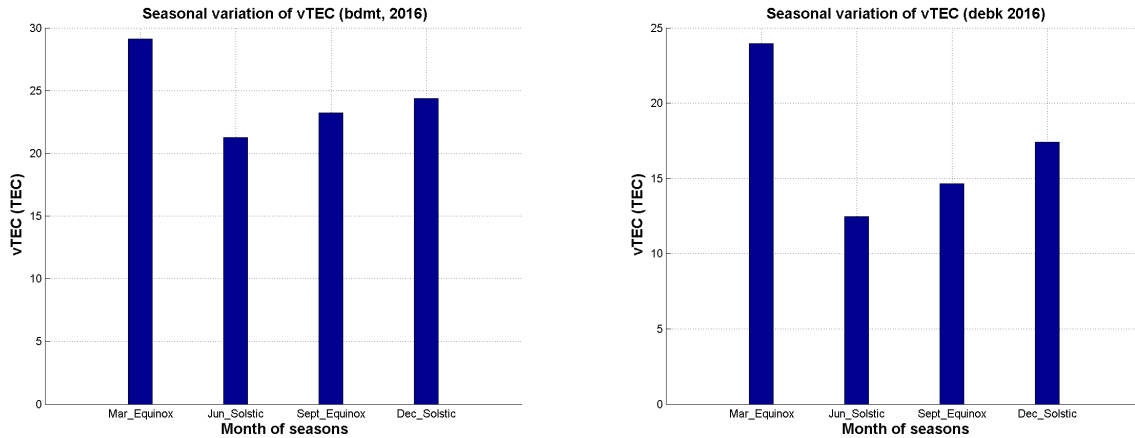


Figure 4.8: Seasonal variation of vTEC at BDMT and DEBK stations

water vapor and multipath effect.

The left panel of Figure 4.8 shows the seasonal variation of vTEC at BDMT station. As observed from these figure, the peak vTEC values observed during March equinox approximately 29.12 (TECU) and the last vTEC values were observed during June solstice approximately 21.26 (TECU). It can also be see from the right panel of this Figure the seasonal variation of vTEC over DEBK station, since the maximum value of vTEC were recorded during March equinox approximately 24 (TECU) while the last vTEC values also observed during June solstice approximately 12.46 (TECU). Figure 4.9 represents the seasonal variation of vTEC at NEGE and KASM stations. As observed from the left panel of these Figure, the peak vTEC values recorded during March equinox around 22.18 (TECU) while the last vTEC values observed during June solstice approximately 13.67 (TECU) at NEGE station. The right panel of Fig. 4.9 shows the seasonal variation of vTEC at KASM station. As observed from these Fig, the maximum value of vTEC observed during March equinox approximately 13.77 (TECU) while the minimum val-

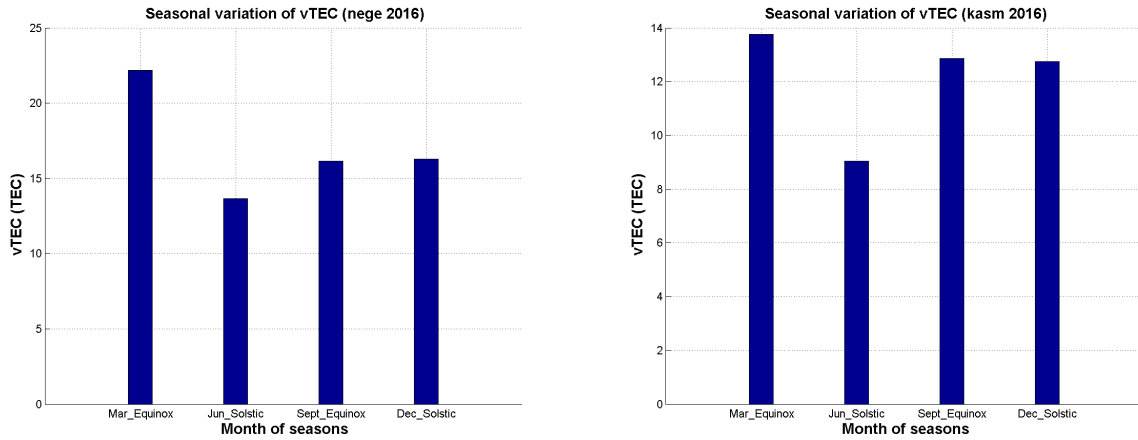


Figure 4.9: Seasonal variation of vTEC at NEGE and KASM stations

ues of vTEC were observed during June solstice approximately 10 (TECU). It is revealed that the highest values of vTEC are generally observed over BDMT and DEBK stations during the norther hemisphere while the lowest values observed NEGE and KASM stations (due to geomagnetic coordinate) during southern hemisphere while the station located far from the equator the highest value of vTEC are observed in December solstices than June solstices due to asymmetric trans-equatorial neutral wind from summer to winter. This result indicates that the rise of the electron concentration in winter than in summer solstice. Generally, the seasonal variation of vTEC values during the equinox are observed to be higher than that of solstice over all stations. This observation can be attributed to the fact that during the equinox, the Sun is directly overhead at the equatorial region thus resulting in higher ionization over this region. However, for DEBK and NEGE stations the variation of vTEC value is slightly maximum during December solstic than September equinox. This observation is reported by (Rama Rao et al., 2006; Yekoye, 2015; Kassa et al., 2015) and contradicted with (Venkata et al, 2017). It may also be resulting due to

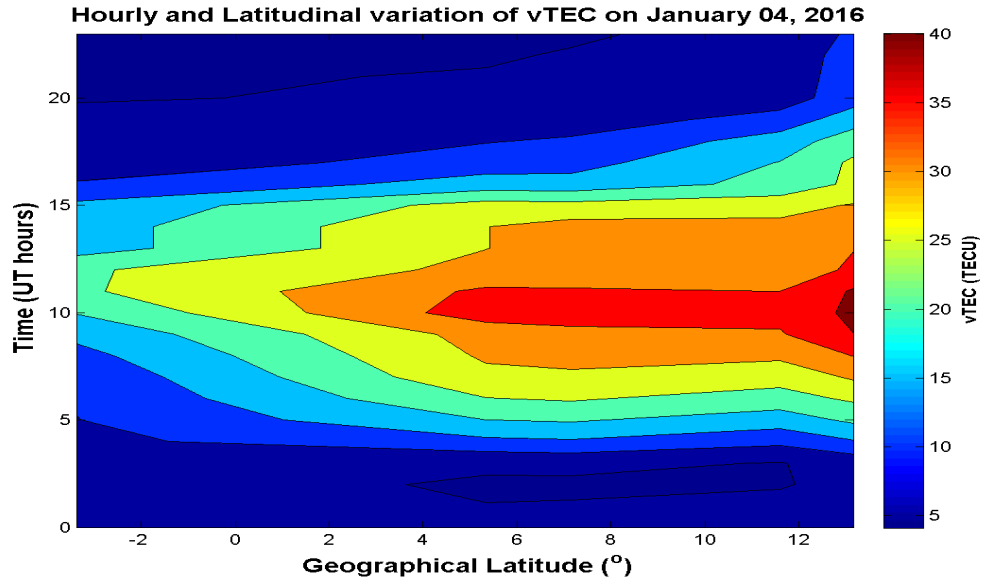


Figure 4.10: The diurnal variation of ionospheric vTEC as a function of latitude during 04 January, 2016

the variations of the solar zenith angle.

4.6 Latitudinal variation of ionospheric vTEC

In this section we discuss about the variation of TEC as a function of latitude in the East African sector using simultaneous GPS-TEC data from five different station. The ionosphere is a function of latitude and the latitudinal response to the variations also depends on the time of the day.

Figure 4.10 shows the diurnal variation ionospheric vTEC as a function of latitudes over five East Africa regions during 04 January 2016. From the figure, we observed that the maximum diurnal variation of ionospheric vTEC occurs at 12:00 UT and it maximum values recorded approxi-

mately 40 (TECU) at DEBK station while the least values of ionospheric vTEC occurs between 00:00 - 06:00 UT and 17:00 - 23:00 UT at all stations. During January month the sun is tilted to the southern hemisphere it mean that the maximum radiation is occurred in the southern hemispheres and maximum plasma is reached. Due to the temperature gradient the flow of plasma from southern hemisphere into the northern hemispheres. According to [Opio et al. \(2015\)](#); [Kassa et al. \(2015\)](#) studied larger variations of vTEC are observed in daytime. The day time vTEC enhancement particularly at the low latitude depends greatly on the strength of the EIA, as a result of $E \times B$ drift and the consequent diffusion along magnetic field lines due to gravity force and pressure gradient, which form two peaks at low latitude, known as the Equatorial Ionization Anomaly (EIA).

Figure 4.11 represents the contour plots of diurnal variation of vTEC for three quiet days as a function of latitude. The data has been investigated for the three typical quiet day ($A_p=2$) in the year 2016, such as 21 October, 2 December and 4 June representing three seasons of Equinox, Winter and summer, respectively. As we can see from these Figure, the day maximum value of ionospheric vTEC increases from the equator to the anomaly crest region. It may also be see from these figure that the values of vTEC on the Equinoxial day (21th October) is maximum as compared to the value of vTEC on the Winter solstice (2nd December) and Summer solstice (4th June). The maximum variation of vTEC value is occurred from 11:00 - 14:00 UT and around the geographical latitudes of 4° to 13° N recorded at about 35 (TECU) on the equinoxial, 29.3 (TECU) during Winter and 28.45 during summer solstice days of 21th October, 2nd December and 4th June, respectively. Such observations were also reported by [\(Rama](#)

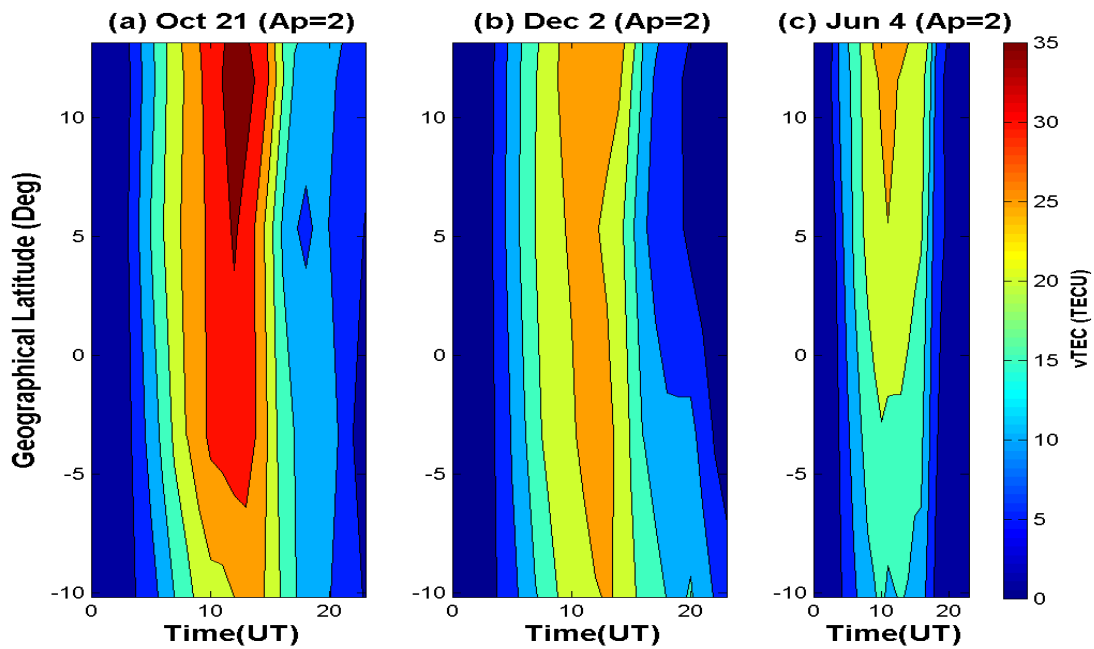


Figure 4.11: Typical quiet days contour plots of the diurnal variations of TEC, drawn as a function of geographic latitude at five stations (DEBK, BDMT, NEGE, ARSH and KASM) for an equinoxial day, 21 October 2016, a winter day, 2 December 2016 and a summer day, 4 June 2016

Rao et al., 2006; Zhenzhoget al., 2012). The reason for due to the fact that the equatorial and low latitude ionosphere is characterized in terms of latitudinal of ionization by a trough at the magnetic equator and crests at about ± 17 magnetic latitude, a feature referred to as the equatorial ionization anomaly (EIA). The peak vTEC values recorded in the equinoctial months can be attributed to have been caused by changes in the sun's position. During equinoctial months, the sun is overhead the equator and temperature at the equator are hotter than at the pole. This makes thermospheric meridional wind blow towards the poles from the equator. This meridional wind changes the neutral composition and O/N₂ ratio increases at equatorial and low latitude regions (due to stronger effect of wind transport during high solar activity). Thus indicates that the maximum variability of vTEC during equinoxes, equatorial ionization anomaly is expected to be more developed than during the solstices. During winter, the duration of day is shorter than summer days. Hence, the production rate of the electrons reaches its peak earlier in winter when compared to summer months. The reason for the lowest values of vTEC during June (summer) solstice is the reduced recombination rate of electrons during winter due to asymmetry in the heating of hemispheres, which causes the transfer of neutral winds from summer to the winter hemisphere, in the summer hemisphere, plasma moves upward along the geomagnetic field lines, while plasma moves downward in the winter hemisphere. Therefore, the transport of the lifted plasma toward the winter hemisphere is enhanced, and the plasma transport toward the summer hemisphere is decreased. The daytime maximum values of vTEC observed in all seasons is as a result of the production processes due to increase in solar EUV fluxes during the daytime in all the season while the minimum values of vTEC observed during nighttime in all seasons can be

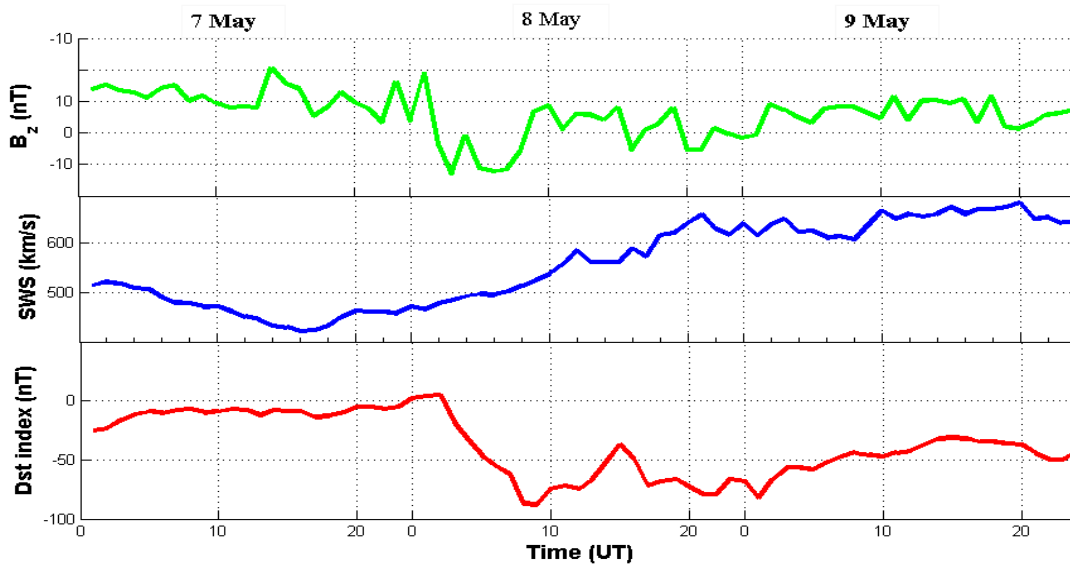


Figure 4.12: Diurnal variation of geomagnetic indices on May 7 - 9, 2016

due to the recombination process.

Fig. 4.12 illustrates the diurnal variation of geomagnetic indices on May 7 - 9, 2016 and Figure 4.13 represents the latitude variation of ionospheric TEC during the storm event (May 7 - 9, 2016) at BDMT, DEBK, NEGE, KASM and ARSH, situated at varying latitudes in the equatorial anomaly East Africa region.

On May 07, the peak storm was reached at 14:00 UT with the solar wind speed values of 433 km/s, the northward IMF Bz values of 5.3 nT and Dst index with a value of -8 nT and its maximum ν TEC values is reached at about 34.7 (TECU) (BDMT). During this time the ionospheric variability seen in low latitude it caused by the compression of the front of the magnetosphere with the arrival of a burst of solar plasma and the Earth's magnetic field remains strong.

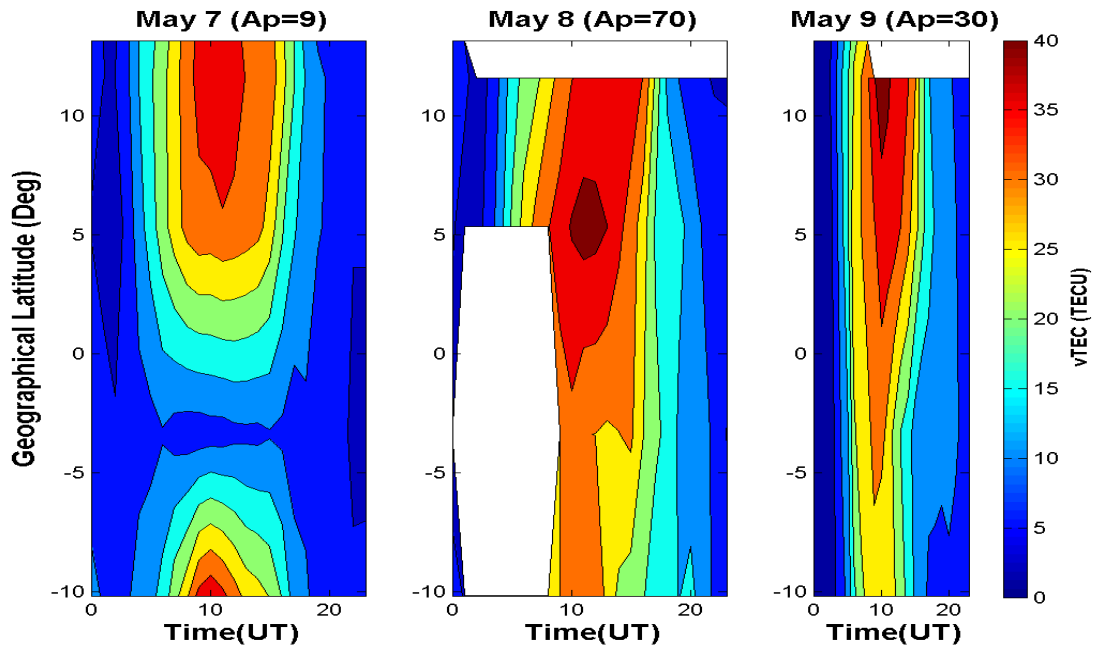


Figure 4.13: Typical contour plots of the diurnal variations of TEC, drawn as a function of geographic latitude at five stations (DEBK, BDMT, NEGE, ARSH and KASM) during geomagnetic storm

On May 8, the storm were occurred at 33:00 UT with the solar wind speed value of 524km/s, the southward IMF Bz value of -1.500nT and the Dst index value of -88 nT and its peak vTEC values is reached at about 34.57 (TECU) (NEGE) and thus indicates that the variation of ionospheric vTEC were occurred greatly at low latitude of ionosphere and it develops over a period of a few hours to a day.

On May 9, the storm occurs around 03:00 UT in the solar wind speed values of 649 km/s with the northward IMF Bz and the Dst index reaches at about -18 nT and the value of vTEC are minimum it is about 3.42 (TECU) (KASM). Due to the results from a decrease in the ring current plasma when the source is terminated and the existing plasma lost by various mechanisms. During this time, the double-hump structure of the EIA was weak and the overall ionization was lower compare to the period before the storm time, which causes the vertical and pole-ward transport of the equatorial plasma. If the zonal electric field is reversed to westward direction, a reversed fountain can occur. Hence from this it can be conclude that the variation of vTEC depends on the activity of Sun and the geomagnetic activity but during geomagnetic activity the variation of vTEC can be depend on times which is an energetic charged particle reaches in the Earth's magnetosphere.

Generally, the ionosphere is primarily affected due to solar radiations. An energetic charged particles, like solar flare, CME's and solar wind are emitted from the sun. This radiation is a consequence of geomagnetic storm. A geomagnetic storm usually starts with increased intensity of Earth's magnetic field called the initial phase, followed by a large decrease termed as the main phase, and the subsequent period of recovery phase. Effects of the geomagnetic storms on the

ionosphere are more severe over the aurora zone (high latitude), but the consequences are more complex in the equatorial anomaly (low latitude) regions caused by the prompt penetration of interplanetary electric field (PPE) and the disturbance dynamo. PPE is also produced by during the southward turning of the interplanetary magnetic field (IMF) B_z known as Under shielding electric field and also during the terminating phase of the substorm when IMF B_z turns northward known as over shielding electric field. The southward turning of B_z produces the eastward or westward electric current during the day and night times respectively, while the northward turning B_z produces the westward or eastward electric field during the day and the night times, respectively. Thus, during daytime, it enhances the daytime eastward zonal electric field over equatorial latitudes, this result in the uplifting of plasma to higher altitudes over the equator and extension of equatorial ionization anomaly (EIA) towards the farther lower latitudes. Thus higher TEC values at low latitudes during the day sector. The reverse of the process takes place during the nighttime leading to the depletion in TEC. In general the PPE from high to low latitudes takes place with sudden southward turning of IMF and rapid changes in the magnetospheric convection. Ionospheric disturbance dynamo electric field produced by the global thermospheric wind circulation due to energy input at polar regions. This occurs mainly during the onset or main phase of the storm. Further, the storm-time EIA can also be influenced by changes in the thermospheric composition, which determines the production and loss rates of the ionospheric plasma (Richa et al. , 2011; Zhao et al., 2005).

CHAPTER 5

Conclusions and Recommendations

5.1 Conclusion

In this study we have used the GPS-TEC data from five East Africa sectors and to investigate the variation of ionospheric $vTEC$ in terms of diurnal, day to day, monthly, seasonal and latitudinal variations during maximum solar activity period in the year 2016. The result showed that the diurnal variation of $vTEC$ reaches its maximum value during daytime around from 1000UT to 1500 UT and minimum value during presunrise around from 0000 UT to 0300 UT and after sunset. In addition, the maximum values of monthly and seasonal variation of $vTEC$ are observed during March equinoctial months while minimum values of $vTEC$ has observed during June solstice's months. Further the latitudinal variation of ionospheric $vTEC$ are also observed. Hence it can be conclude that the maximum variation of $vTEC$ values have recorded in the low latitude/equatorial region. The equatorial and low latitude ionosphere is characterized by the existence of the daytime Equatorial Ionization Anomaly (EIA). The EIA is produced by the equatorial ionospheric fountain effect at the dip equator which is formed by daytime eastward electric fields. The eastward electric fields together with the almost horizontal northward directed B-field produce an upward $E \times B$ vertical drift which lifts the plasma to higher altitudes from where it diffuses to

higher latitudes along magnetic field lines. The diffusion of the plasma to higher latitudes creates ionization crests on both sides of the magnetic equator at about $\pm 15^\circ$ magnetic latitudes. And, the latitudinal variation of vTEC during geomagnetic storm on 7-9 May 2016 was done. Our result shows that the maximum variation of vTEC are observed during initial phase rather than the main phase and the recovery phases. This conclusion becomes due to the time of the storm reaches to the Earth's magnetosphere.

5.2 Recommendation

Since ionosphere is a very complex dynamic environment. But the variation of ionospheric electron density depends on latitude, longitude, altitude, solar and geomagnetic activities. So in the future work, we recommended that it should be make the variation of ionospheric TEC using different modeling over East Africa and also it should be considering the mathematical expressions. Our future work will concentrate on investigating the spatial variation of ionospheric TEC by using different modeling.

References

Adolph s. Jursa, 1985. Handbook of geophysics and the space environment, United State Air Force.

Brekke. A, 1997. Physics of the Upper Polar Atmosphere, 2nd Edition

Olwendo O. J., Baki P., Mito C. and Doherty P, 2012. Characterization of ionospheric GPS Total Electron Content (GPSTEC) in low latitude zone over the Kenyan region during a very low solar activity phase. Journal of Atmospheric and Solar-Terrestrial Physics, 84 - 85(0).

Hunsucker, R., and Hargreaves . J, 1995. The high latitude Ionosphere and its effect on Radio propagation. Cambridge University Press.

Davies, K , 1990. Ionospheric Radio, Peter Peregrinus, London, *Adv. Space Res*, **42**, 720 - 726.

Garner, T. W, Gaussiran II, Tolman. B, Harris. B, Calfas. 's and Gallagher. H, 2008. Total electron content measurements in ionospheric physics, *Adv. Space Res*, **42**, 720 - 726

Hanslmeier. A (2007). The sun and space weather, 2nd Edition, **347**

Tascione. F, 1988, Introduction to the space environment, 2nd Edition

Moldwin. M, 2008. An introduction to space weather, Cambridge University press.

- Olawepo. O, Adeniyi. O, and Oluwadare. J, 2017. TEC variations and IRI-2012 performance at equatorial latitudes over Africa during low solar activity, *Advances in Space Research*, **59**, 1800 - 1809, <http://www.sciencedirect.com>
- Yekoye A. T, 2015. Comparison of GPS-TEC with IRI-2012 TEC over African equatorial and low latitude regions during the period of 2012-2013 and Pattern of GPS-TEC variation over low-latitude regions (African sector) during the deep solar minimum (2008 - 2009) and solar maximum (2012 - 2013) phases, *Advances in Space Research*, **56**, 1677 - 1685, <http://www.sciencedirect.com>
- Kassa. T, Samson. T, and Baylie. D, 2017. Solar activity indices as a proxy for the variation of ionospheric Total Electron Content (TEC) over Bahir Dar, Ethiopia during the year 2010 - 2014, *Advances in Space Research*, **60**, 1237 - 1248, <http://www.sciencedirect.com>
- Goodman. M, 2005. Space weather and telecommunications, Radio Propagation Services, Inc. (RPSI) Alexandria VA 22308 - 1943
- Klobuchar. A, 1996. Ionospheric effects on GPS. In: Spilker, J.J., Parkinson, B.W. (Eds.), *Global positioning system: theory and applications*, 485 - 515
- Hamzah. M and Homam. J, 2015. The correlation between total electron content variations and solar activity *ARPJN Journal of Engineering and Applied Sciences*, **10**, 1819 - 6608, <http://www.arpnjournals.com>

- Negasa. A, Kasam. S, Damtie. B, Nigussie. M, and Raghavendra. T, 2015. Reaction of Ethiopia Ionosphere to Sun based Movement and Geomagnetic Storm *International Journal of Modern Chemistry and Applied Science*,**2(4)**, 228 - 234
- Galav P. N. Dashora, S. Sharma, and R. Pandey, 2010. Characterization of low latitude GPS-TEC during very low solar activity phase,*J. Atmos. Sol. Terr. Phys.*, **72**, 1309 - 1317.
- Kumar. S and Singh. K. A (2009), Variation of ionospheric total electron content in Indian low latitude region of equatorial anomaly during May 2007-April 2008,*Adv. Space Res.*, **43**, 1555 - 1562.
- Rama Rao. P. V, Gopi Krishna. S, Niranjana. K and Prasad. D, 2006. Temporal and spatial variations in TEC using simultaneous measurements from the Indian GPS network of receivers during the low solar activity period of 2004-2005, *Ann. Geophys*, **24**, 3279 - 3292, <http://www.ann-geophys.net.24.3279.2006>.
- Oron. S, Ujanga. F. M and Ssenyanga. T. J, 2013. Ionospheric TEC variations during the ascending solar activity phase at an Equatorial station, Uganda, *India Journal of Radio and space physics.*, **42**, 7 - 17
- Michael, c. Kelley(2009),The Earth's Ionosphere Plasma Physics and Electrodynamics, International Geophysics Series, *Academic Press, inc.*
- Adeniyi. J, 2008. Subduing the Earth: The Ionosphere Inclusive 85th inaugural lecture. University of Ilorin, Nigeria.

- Adewale. A, Oyeyemi. E, Adeniyi. J, Adeloye. A and Oladipo. O, 2011. Comparison of total electron content predicted using the IRI-2007 model with GPS observations over Lagos, Nigeria. *Indian J. Radio Space Phys*, **40**, 21 - 25.
- Opio. P, Dujanga. M. F, and Ssenyonga. T, 2015. Latitudinal variation of the ionosphere in the African sector using GPS TEC data *Advances in Space Research* **55** , 1640 - 1650,
- D. Venkata Ratnam, G. Sivavaraprasad, N. S. M. P. Latha Dev, 2017. Analysis of ionosphere variability over low-latitude GNSS stations during 24th solar maximum period, *Advances in Space Research*, **60** , 419 - 434
- Olwendo. J. O, Baki. P, Mito. C and Doherty. P, 2012. Characterization of ionospheric GPS Total Electron Content (GPS-TEC) in low latitude zone over the Kenyan region during a very low solar activity phase, *Journal of Atmospheric and Solar-Terrestrial Physics* 84 - 85
- Kshudiram. S, 2008. The Earth's Atmosphere, University Park, USA
- Kassa. T, Damtie. B, Bires. A, Yizengaw. E, and Cilliers. P, 2015. Spatio-temporal characteristics of the Equatorial Ionization Anomaly (EIA) in the East African region via ionospheric tomography during the year 2012, *Advances in Space Research*, **55** 184 - 198
- Olwendo. J, Yosuke. Y, Cilliers. J. P, Baki. P and Doherty. P, 2016. A study on the variability of ionospheric total electron content over the East African low-latitude region and storm time ionospheric variations, *Radio Sci.*, **51**, <http://www.doi:10.1002/2015RS005785>.

- Olawepo. O. A, Adeniyi. O. J, and Oluwadare. J. E, 2017. TEC variations and IRI-2012 performance at equatorial latitudes over Africa during low solar activity, *Advances in Space Research*, **59**, 1800 - 1809
- Ratnam. V. D, Sivavaraprasad. G and Devi. L. P. M. S. N, 2017. Analysis of ionosphere variability over low-latitude GNSS stations during 24th solar maximum period, *Advances in Space Research*, **60**, 419 - 434
- Malini. A, Joshi. P. H, Iyer. N. K, Kwak. S. Y, Lee. J. J, Chandra. H, and Cho. S. K, 2012. Day-to-day variability of equatorial anomaly in GPS-TEC during low solar activity period, *Advances in Space Research*, **49**, 1709 - 1720
- Kelley. M. C, '1989. The Earth's ionosphere plasma physics and electrodynamics, 1st Edition. *International Geophysics Series*, **43**.
- Richa. T, Amit. J, Sudhir. J and Gwal. K, 2011. Study of TEC changes during geomagnetic storms occurred near the crest of the equatorial ionospheric ionization anomaly in the Indian sector, *Advances in Space Research*, **48**, 1617 - 1630
- Xu Zhenzhong. X, Weimin. W, Nan. Z, Xiaofei. S and Haotian. Z, 2012. Variability study of ionospheric total electron content at crest of equatorial anomaly in China from 1997 to 2007, *Advances in Space Research*, **50**, 70 - 76
- Zhao, B. , Wan, W. and Liu, L., 2005. Responses of equatorial anomaly to the October-November 2003 super storms. *Ann. Geophys.* **23**, 693 - 706.

- Yinn, N., Kang, C. and Sen, W. 1989. On the equatorial anomaly of the ionospheric total electron content near the northern anomaly crest region. *J. Geophys. Res.*, **94** (A10).
- Banks, P. M., R. W. Schunk, and W. J. Raitt, 1976. The topside ionosphere: A region of dynamic transition, *Annl. Rev. Earth Planet. Sci.*, **4**, 381
- Win. Z. H. , Yoshitaka. G , Yoshiya. K, 2016. Estimation Method of Ionospheric TEC Distribution using Single Frequency Measurements of GPS Signals, *International Journal of Advanced Computer Science and Applications*, **7 (12)**